

Archive ouverte UNIGE

https://archive-ouverte.unige.ch

Thèse 2016

Open Access

This version of the publication is provided by the author(s) and made available in accordance with the copyright holder(s).

Role of lipids in COPII vesicle formation

Melero Carrillo, Alejandro

How to cite

MELERO CARRILLO, Alejandro. Role of lipids in COPII vesicle formation. Doctoral Thesis, 2016. doi: 10.13097/archive-ouverte/unige:85258

This publication URL: https://archive-ouverte.unige.ch/unige:85258

Publication DOI: <u>10.13097/archive-ouverte/unige:85258</u>

© This document is protected by copyright. Please refer to copyright holder(s) for terms of use.

Role Of Lipids In COPII Vesicle Formation

THÈSE

présentée à la Faculté des sciences de l'Université de Genève pour obtenir le grade de Docteur ès sciences, mention biochimie

par

Alejandro MELERO CARRILLO

de

Séville (Espagne)

Thèse Nº 4896

GENÈVE

Atelier Repromail
Année
2016



Doctorat ès sciences Mention biochimie

Thèse de Monsieur Alejandro MELERO CARRILLO

intitulée :

"Role of Lipids in COPII Vesicle Formation"

La Faculté des sciences, sur le préavis de Monsieur H. RIEZMAN, professeur ordinaire et directeur de thèse (Département de biochimie), Monsieur A. ROUX, professeur associé et codirecteur de thèse (Département de biochimie), Monsieur J. GRUENBERG, professeur honoraire (Département de biochimie) et Monsieur B. ANTONNY, docteur (Institut de pharmacologie moléculaire et cellulaire, Valbonne, France), autorise l'impression de la présente thèse, sans exprimer d'opinion sur les propositions qui y sont énoncées.

Genève, le 3 février 2016

Thèse - 4896 -

Le Décanat

Index

Acknowledgments1
Summary3
Chapter I: The role of lipid structures in membrane deformation
Chapter II: Defects in COPII vesicle formation are rescued by phospholipase overexpression23
Chapter III: Lipidomic analysis reveals that COPII vesicles are enriched in lysophospholipids35
Chapter IV: COPII proteins binding to artificial liposomes is enhanced by lysophospholipids44
Chapter V: Discussion and conclusions51
Chapter VI: Materials and methods54

Acknowledgments.

This work was supported by the National Centre of Competence in Research in Chemical Biology, funded by the Swiss National Science Foundation and by the University of Geneva. I would like to express my sincere gratitude to all the people that in one way or another helped me to carry out this project. First I would like to thank both Howard Riezman and Aurélien Roux for giving me the chance to take this challenging project, for their support, guidance and advice; I could not have asked for more. Also, I would like to thank all of my labmates (past and present) for their advice, supporting criticism and assistance; not to mention it is always easier to work surrounded by such friendly and creative people. I would like to thank as well Jean Gruenberg and Bruno Antonny as it is an honour to have their evaluation and contribution to this project. Finally, I would like to express my thankfulness to all the members of the Biochemistry Department for their support, advice and kindness every single day during these years, including weekends and holidays.

In addition, I would like to give special thanks to Charles Barlowe for his generous support and discussions, since with no doubt those days at Dartmouth were crucial for this project and also a great experience. Thanks as well to Akihiko Nakano for generously sharing yeast strains and advice. My gratitude as well to Kouichi Funato and collaborators since their observations made possible this wonderful project. Thanks as well to Robbie Loewith for his advice and support and to Christoph Bauer for his technical support and assistance.

Since a scientist does not only need good observations to successfully complete a project, I would like give thanks to many people that made hard work look easy just by being there when I needed them. Without a doubt, I would like to thank my parents and brother for their unconditional support and affection, regardless of the day or the hour, a las duras y a las maduras. In a like manner, I can not find the words to give thanks to Auxiliadora Aguilera, for her scientific advice, fruitful discussions (even those close to violence) and for all those materials of which, if I do a list, someone may accuse me of plundering her bench. My deepest gratitude to Aline Santos, for not letting our friendship get in the way of a thoughtful criticism when I was showing her a not-so-clear piece of data. Moltes gràcies to Adai Colom for highly inspirational coffee times, beer times, late hour work times, microscopy times and overall his friendship. Eskerrik asko to Noemi Jiménez, for all the good moments, quarrels and unconditional support. Also for not accepting an unclear ugly graph ever, regardless of the data. I would like to thank as well Ana Teresa López for her friendship and her support; always since those biochemistry classes. I would like to give special thanks to Annika Hohendahl, Frédéric Humbert, Guillaume Molinard, Nicola Chiaruttini, Saleem Mohamed

and Sandrine Morlot for making laboratory 341 a very nice working environment as well as one of the amusing places ever to exist at the Faculté des Sciences.

Last but not least, I would like to thank all the good people and friends I made in Geneva, as well as my old good friends from Sevilla, because they contributed to this work by granting me five wonderful years with plenty of good moments, in Geneva and from the distance.

Finally, I would like to dedicate this work to Jose María Gómez Alcaide, Josefina Hidalgo and Enrique Cerdá, because their classes taught me the most important aptitudes for science: dedication and passion.

Résumé.

A l'intérieur de la cellule, le transport des protéines et des lipides entre les organelles est réalisé par des transporteurs membranaires appelés vésicules. La formation de ces vésicules nécessite la participation de protéines d'enveloppe qui sont capables de changer la forme des membranes en les courbant. Finalement pour libérer les vésicules dans le cytoplasme, la coupure du cou qui les relient à la membrane est nécessaire. Le transport vésiculaire à partir du réticulum endoplasmique (RE) vers l'appareil de Golgi est réalisé par des protéines du complexe Coat Protein II (COPII). Les vésicules COPII sont formées dans des zones appelées sites de sortie du RE (ERES en anglais). Ce complexe des protéines s'attache séquentiellement à la membrane. Initialement, la protéine transmembranaire Sec12 recrute la petite GTPase Sar1 qui, une fois liée au GTP, libère une hélice amphiphile qui se lie à la membrane de l'ER. Puis l'hétérodimère Sec23/24 est recruté à la membrane, en coordination avec Sar1 et les protéines forment un complexe de 'pré-bourgeonnement'. Enfin, l'hétérotétramère Sec13/31 s'assemblent sur le complexe de 'pré-bourgeonnement' et finalise la formation dans la vésicule. La dernière étape nécessite la séparation de la vésicule de la membrane du RE, un processus encore mal caractérisé mais dépendant de Sar1. De même, le rôle des lipides dans la déformation des membranes du RE est largement inconnu.

Dans cette étude, je montre comment les lipides participent à la formation des vésicules COPII dans Saccharomyces cerevisiae. Une mutation qui affecte les protéines qui recrute COPII, sec12-4, peut être sauvée par la surexpression de phospholipases, des enzymes qui hydrolysent les glycérophospholipides en lysophospholipides et acides gras libres. Les lysophospholipides sont coniques et leur accumulation induit des changements dans la fluidité de la membrane et dans sa courbure spontanée. Une analyse lipidomique révèle que les lysophospholipides s'accumulent dans les mutants sec12-4 surexprimant des phospholipases. En outre, les vésicules COPII générées in vitro ont été analysées par spectrométrie de masse. Fait intéressant, ces vésicules contiennent quatre fois plus de lysophospholipides que la proportion de lysophospholipides présents dans le RE. Enfin, des reconstitutions in vitro ont été utilisées pour explorer l'effet des lysophospholipides sur la liaison de protéines COPII à des liposomes artificiels. Les images de microscopie confocale révèlent que des liposomes ayant 10% de lysophospholipides permettent plus de liaison de Sec13/31 à la membrane.

Les résultats obtenus dans cette étude établissent une nouvelle connexion entre la formation des vésicules COPII et les lysophospholipides. Leur forme conique peut causer

des changements extrêmes dans la rigidité de la membrane ou des défauts d'assemblage des lipides et ainsi aider les manteaux COPII à déformer la membrane du RE.

Summary.

Inside the cell, transport of proteins and lipids between organelles is mediated by membrane carriers known as vesicles. The formation of these vesicles requires the participation of coat proteins which are capable to change the shape of membranes into extremely curved structures, ultimately catalyzing the scission and release of a free vesicle to the cytoplasm. Vesicular transport from the endoplasmic reticulum (ER) to the Golgi apparatus is mediated by Coated Protein complex II (COPII). COPII vesicles are formed in discrete areas known as ER exit sites (ERES). This coat complex comprises several proteins which bind sequentially to the membrane. Initially, the transmembrane protein Sec12 recruits the small GTPase Sar1, which on its GTP form release an insert an alpha-helix on the ER surface. Then the heterodimer Sec23/24 is recruited to the membrane, which in coordination with Sar1 and cargo proteins form a pre-budding complex. On a latter step, the heterotetramer Sec13/31 scaffolds over the pre-budding complex and completes membrane deformation to form a bud. The last step requires the scission of the vesicle from the ER membrane, a process that is not yet well characterized but that may depend on Sar1. The lipid requirements to deform the ER membrane are largely unknown.

In this study it has been found a novel link between lipids and COPII vesicle formation in *Saccharomyces cerevisiae*. A mutation that affects COPII proteins recruitment, *sec12-4*, can be rescued by the overexpression of phospholipases, which are enzymes that hydrolyze glycerophospholipids into lysophospholipids and free fatty acids. Lysophospholipids are conical lipids whose accumulation may induce changes in curvature or membrane fluidity. Lipidomics have revealed that lysophospholipids accumulate in rescued *sec12-4 mutants* overexpressing these phospholipases. Furthermore, COPII vesicles have been generated with *in vitro* budding techniques and the lipidome analyzed by mass spectrometry. Interestingly, these vesicles had four fold more lysophospholipids than the the proportion of lysophospholipids present in the ER. Finally, *in vitro* reconstitutions have been used to explore the effect of lysophospholipids on the binding of COPII proteins to artificial liposomes. Confocal microscopy images have revealed that lysophospholipids increase the binding of Sec13/31 to the membrane and affects the organization of the coats over the surface of giant liposomes.

The results obtained in this study establish a new link between lysophospholipids and COPII vesicle formation. Their extreme conical shape may cause changes in membrane rigidity or packing defects and by that help COPII coats to deform ER membrane.

Chapter I:

The role of lipid structures in membrane deformation.

Introduction:

Cellular lipids are a collection of metabolites that have diverse functions, including an essential role in determining the structural properties of membranes, intermediates in carbon and energy metabolism, as well as signal transduction. Although their chemistry is highly diverse, most of them share the common property of being amphipathic (with hydrophilic and hydrophobic parts in the same molecule). This feature allows them to spontaneously organize in various structures, most often in bilayers that separate the cell from its environment (plasma membrane) or organelles from the rest of the cell. The distribution of lipid species among the different cellular organelles is highly regulated (Holthuis and Menon, 2014). Moreover the two leaflets of the bilayer are usually of different composition, a feature called membrane asymmetry (van Meer, 2011).

Strikingly, lipid diversity increases as a function of cellular specialization (Dennis et al., 2010; Pietiläinen et al., 2011; Sampaio et al., 2011). This supports the idea that lipid composition is strongly adapted to the specific function of a cell, and or of an organelle. This functional link between the chemical nature of the lipids and their role in the cell points to the numerous functions of lipids: as signaling molecules, semi-permeable barriers, and active players of lipid membrane remodeling. This chapter focuses on this last aspect, how lipids interact with protein machineries to change or stabilize membrane topology and to which extent this is mediated by lipid shape.

Diversity of lipid structures.

Both bacterial and eukaryotic organisms share glycerophospholipids as major constituents of their membranes. Glycerophospholipids are composed of glycerol, esterified with two acyl chains and a phosphate group (figure 1a). Different species differ in their in acyl chains and/or headgroups. Free acyl chains have a carboxyl group followed by a hydrocarbon chain. They can be attached to the glycerol via an ester or ether linkage. The number of carbons will determine the length of the chain. If there is one or several carbon-carbon

double bonds, the acyl chain is considered unsaturated. The countless possible combinations in length and unsaturation degree generate a great diversity of acyl chains. A glycerophospholipid can be composed of two equal acyl chains, but also two different ones, adding chemical variability to the molecule (figure 1b). The phosphate can be modified by adding diverse hydrophilic structures, such as choline, inositol, ethanolamine or serine. Each molecule will add different chemical characteristics to the glycerophospholipid, such as electrostatic charge.

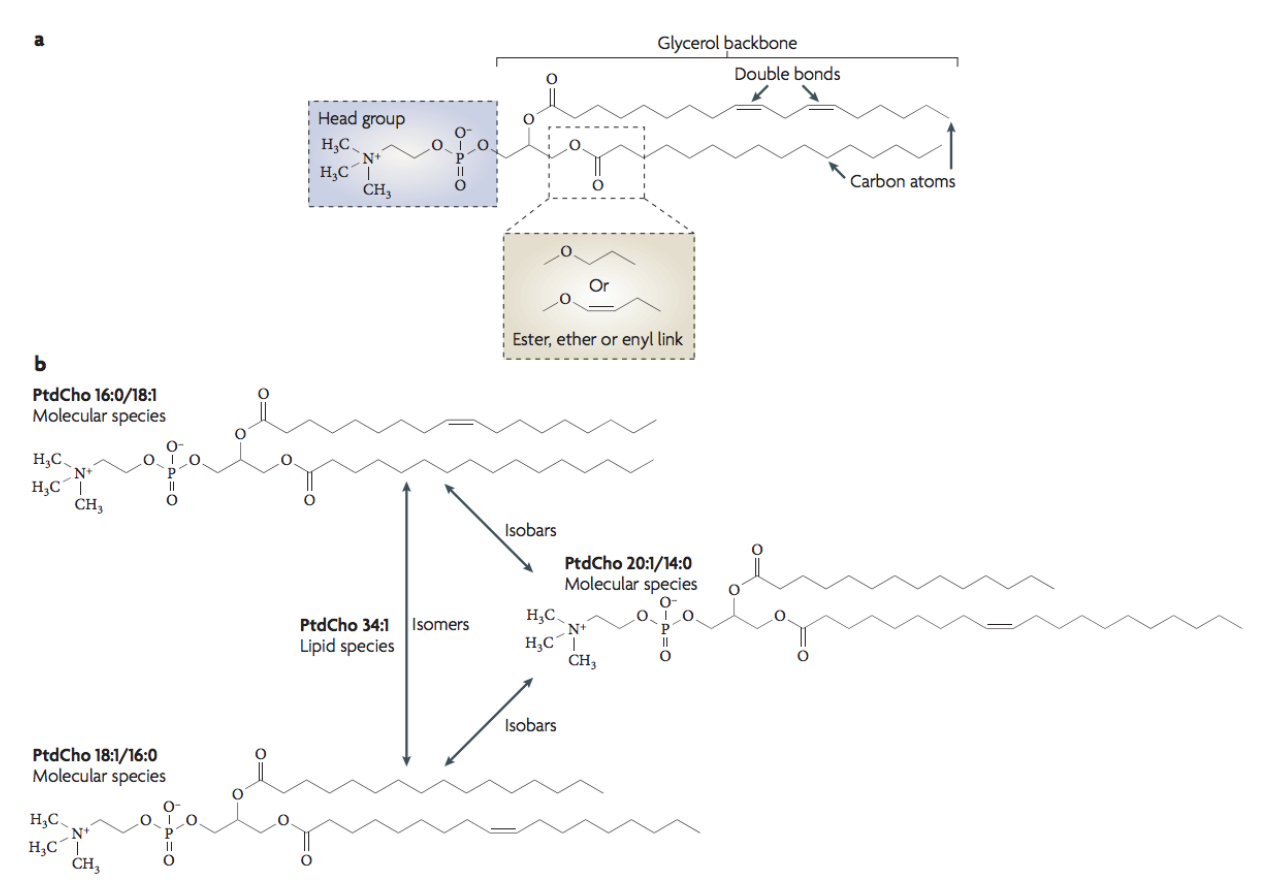


Figure 1. Reproduced from (Shevchenko and Simons, 2010). a) Schematic view of glycerophosphatidylcholine (PC). b) Representation of glycerophospholipid isomers. Different isomers of a PC34:1 with similar acyl chains in different positions. Same amount of carbon atoms in PC molecule can be achieved with different acyl chain composition.

Ceramides and sphingolipids are less abundant but not less important for many cellular processes. In contrast to glycerophospholipids, their structure is based on sphingosine, a long amino alcohol hydrocarbon chain. An amide bond between an acyl chain and sphingosine leads to the formation a ceramide molecule. Ceramides can be later modified with a soluble headgroup, such as phosphocholine, phosphoserine, sugar residues or oligosaccharides.

The last major group of lipids in the cell are sterols, present in most eukaryotes. They are steroid molecules with several hydrophobic carbon rings, usually having a hydroxyl group in

one these rings. Sterols are not as diverse as other lipid classes, being commonly represented by one major species per organism, such as cholesterol in mammalian cells or ergosterol in yeast.

To minimize their energy, amphipathic lipids auto-assemble into various structures that allow for physical separation of the hydrophobic chains and the water. These structures can be micellar (Luzzati et al., 1968) although rare *in vivo*, where the most prominent form is a bilayer (figure 2). This is due to the fact that most of the lipids have a cylindrical shape, which allow for hydrophobic packing of the acyl chains in the flat bilayer. Since lipids have different chemical structures, their shapes (from conical to inverted cone) and physicochemical properties are quite variable.

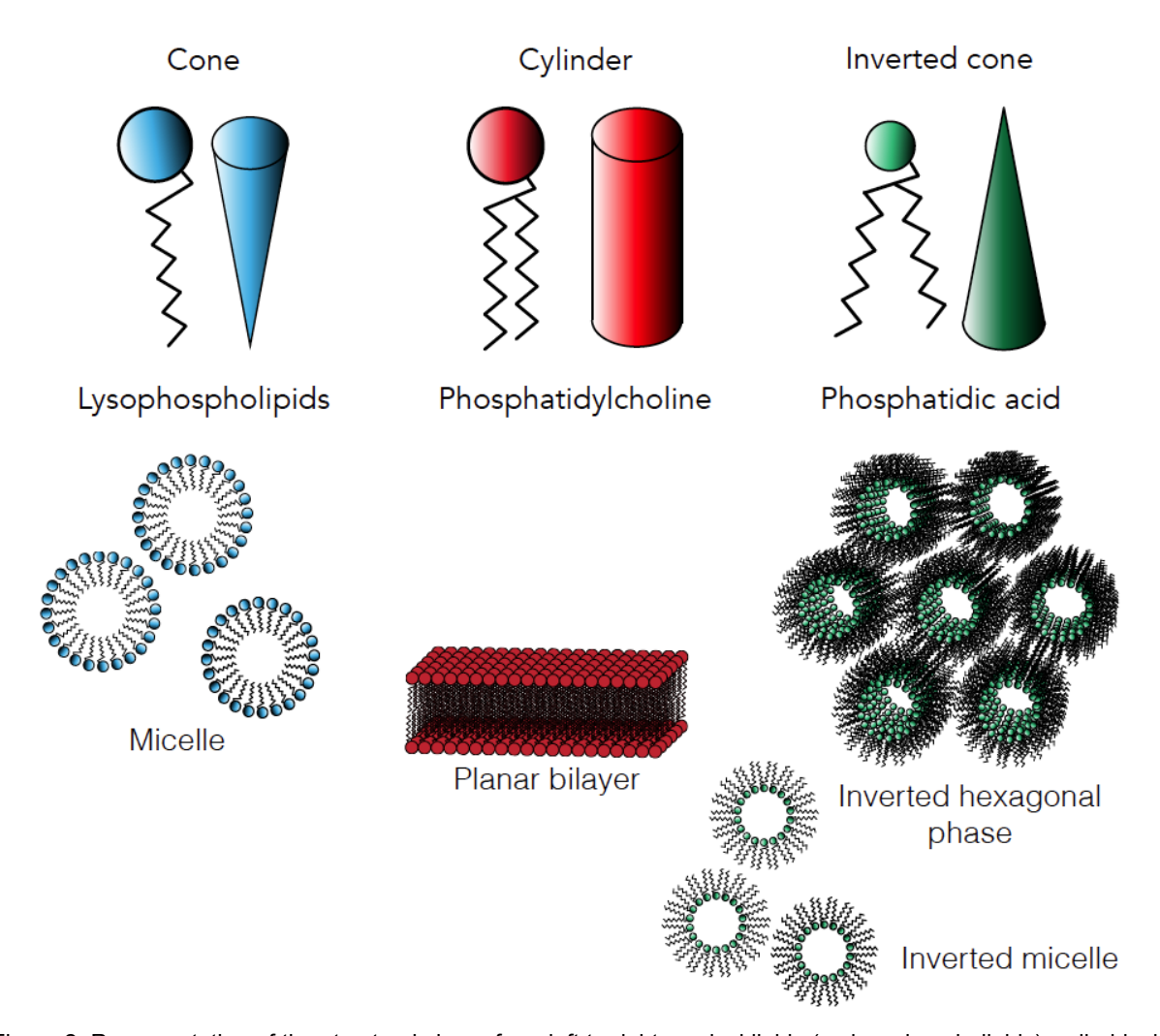


Figure 2. Representation of the structural shape from left to right: conical lipids (as lysophospholipids), cylindrical lipids (as PC), and inverted conical lipids (phosphatidic acid {PA}). Below, different structural organization of lipids: From left to right, micelles, planar bilayers, inverted hexagonal phase and inverted micelles.

How the different shapes of lipids can impact the properties of membranes has been a subject of debate since the pioneering studies with X-ray diffraction (Luzzati et al., 1968). PC

molecules, the main lipid species present in cellular membranes, are known to form planar bilayers because of their rather cylindrical shape: the radius of the choline steric volume is comparable to the radius of the steric cylinder occupied by the 2 acyl chains. On the other hand, lipids with conical shape will generate micellar, tubular or even more complex nonbilayer structures (Tenchov et al., 2012). An example of such lipid is PE: the steric radius of the ethanolamine headgroup is smaller than the divergent angle of its acyl-chains. This can affect the structure of the bilayer since the balance between lipid shapes in both leaflets determines the spontaneous (relaxed) curvature of the membrane (Callan-Jones et al., 2011a). In a monolayer of conical lipids, their optimal packing will induce curvature of the membrane proportional to their shape. Therefore, accumulation of conical shapes could lead to the spontaneous bending of a membrane. In closed bilayers, this curvature is considered positive when the membrane bends towards its outside and negative when it bends towards the inside (McMahon and Gallop, 2005). Some lipids which are proposed to participate in membrane shaping such as phosphatidic acid (PA) or its lyso version LPA are indeed able to induce spontaneous curvature (Kooijman et al., 2005). Membrane curvature or combination of cylindrical and conical lipids in a bilayer will result in irregularities in the geometrical arrangement of lipids, gaps between headgroups and or acyl chains, known as packing defects (Vamparys et al., 2013).

Eukaryotic cells exploit this shape diversity to generate highly specialized membranes. There is great agreement in the literature about asymmetric distribution of lipid species among each different organelle in eukaryotic cells (Schneiter et al., 1999). Although our understanding of this lipid sorting is still poor, there is strong evidence that suggests the existence of distinctive physicochemical regions inside the cell. Clear examples of this are the endoplasmic reticulum (ER) and the plasma membrane. Despite the fact that sterols and ceramides are initially synthesized in the ER, this organelle is mostly composed of unsaturated glycerophospholipids, especially PC, PE and PI, with low amounts of phosphatidylserine (PS). Therefore, the ER surface is presented to the cytosol as a mostly neutrally charged and very fluid membrane.

On the reverse, plasma membrane is usually described as a very ordered membrane, capable of resisting mechanical stresses and control communication of solutes with the external environment. It is enriched in saturated glycerophospholipids (Schneiter et al., 1999) and contains the majority of sphingolipids and sterols of the cell (Patton and Lester, 1991); (Klemm et al., 2009). Sphingolipids are proposed to be asymmetrically distributed to the outer leaflet of plasma membrane, while PS and phosphoinositides have been shown to accumulate in the inner leaflet.

The fluid mosaic model placed lipids and membranes as important players in cell biology (Singer and Nicolson, 1972), but neglected the changes of its properties, in particular its

physical properties, linked to the chemical diversity of lipids, and its inhomogeneous distribution in cells. In this chapter will be discussed how chemical structure of lipids affects the mechanics of lipid membrane.

Shape role in membrane physics.

As described before, lipids tend to organize as a bilayer thanks to their amphipathic characteristics. Although the thickness of the bilayer is on the range of 3-4 nm, the surface of the membrane is not necessarily restricted, being possible surfaces of several of micrometers. Because lipid molecules can easily diffuse in the plane of the membrane, lipid bilayers are often described by physicists as two-dimensional fluids. This allows us to approximate the mechanical properties of membranes. A membrane can be deformed in two ways: by changing its surface area or by changing its curvature. Compressive and pulling forces will change its surface area. Bilayers have limited compressibility, thus its expansion or compression is limited under stretching or compressive forces respectively (not more than 10% area expansion or compression). However, stretching forces will increase the tension of the membrane. Once these stretching forces are stopped, the membrane can recover its original shape, evidencing an elastic behavior (Evans et al., 1987). At constant temperature, the resistance to stretching or pulling forces for a given membrane composition will depend on the compressibility of that mixture, which can be expressed as the area compressibility modulus (χ) . High χ values correspond to less elastic membrane compositions, generally difficult to stretch, as sphingolipids or saturated phospholipids. Low χ values correspond membranes with higher elasticity, which can be stretched applying less force. Generally, mixtures with unsaturated phospholipids will have low χ values. Membrane elasticity can impact the assembly of coats over membranes. Tension opposes to the polymerization of clathrin onto giant unilamellar vesicles (GUVs), meaning that low tension allows deeper deformations by clathrin coats than at higher tensions, where only shallow deformations can be observed (Saleem et al., 2015).

The second type of deformation is bending. The curvature elasticity of a membrane depends on the deformability of the lipid mixture. The energy needed to deform the membrane is known as bending rigidity, which is measured empirically (Callan-Jones et al., 2011b). Generally, long saturated phospholipids and sphingolipids tend to rigidify membranes. Short chains and unsaturations soften the membranes. Low bending rigidity membranes allows the formation highly curved structures (Roux et al., 2005), which is relevant for the formation of transport intermediates and tubules.

The length of lipid molecules will also affect the thickness of the membrane. Lipids with long saturated acyl chains increase the membrane thickness. Interestingly, unsaturations barely impacts the thickness of the bilayer (Lewis and Engelman, 1983). In summary, the visco-

elastic properties of the bilayer, compressibility and rigidity, will depend on its composition (acyl chain length and saturation) and external forces (tension or bending deformations).

But changes in lipid chain length is also responsible for changes of lipid phase state: stabilized domains have been observed in artificial membranes by modulating temperature or lipid composition, meaning that different lipids can segregate laterally in favourable thermodynamic conditions (Ipsen et al., 1987). In fact, in vitro approaches have shown that these phases can be stabilized at room temperature (Dietrich et al., 2001). In model membranes with ternary mixes, cholesterol and sphingomyelin are able to form a low entropic phase known as liquid order phase (L_o). Water has less penetration inside this phase. Moreover, unsaturated glycerophospholipids (such as dioleyl PC) are excluded from these domains, thus forming another domain called a liquid disorder phase (L_a) . The latter is characterized by a higher entropic regime and more penetration of water inside the bilayer. These phases are discrete domains with lower bending rigidity and different bending capabilities (Baumgart et al., 2003). Not surprisingly, membrane phase separation is seen by many as a potential lipid and protein sorting mechanism along the secretory pathway by segregating specific lipids and proteins into patches called "lipid rafts". Cells can exhibit large membrane inhomogeneities after treatments causing cholesterol depletion (Hao et al., 2001), similar to those seen in artificial membranes with visible phase separation. However, these treatments do not seem to perturb the distribution of GPI-anchored proteins, as would be expected from lipid raft disruption. Genetic and lipidomic studies in S. cerevisiae suggest that sphingolipid and sterols must function together, but not necessarily as a raft (Guan et al., 2009). Moreover, secondary-ion mass spectrometry images show a certain degree of spatial segregation of sphingolipids among homogeneous distribution of sterols across the plasma membrane (Frisz et al., 2013). Large scale computer simulations support these observations and open the possibility of nano-scale transitorial L_0 phase interactions between sterols and highly packed lipids (Ingólfsson et al., 2014).

Interestingly, lipid sorting can be induced upon membrane deformation out of homogeneous membranes (Roux et al., 2005). Tubular deformations, such as those produced by molecular motors such as kinesins exhibit a different lipid composition compared to the donor membrane. It is important to mention that curvature-dependent lipid sorting only happens with membrane compositions close to phase transition. Therefore, the lipid composition with specific shapes could modulate membrane properties. This could be use by protein machineries to deform membranes into extremely curved vesicles. Possibly, proteins could interact with lipids, inducing local lipid sorting to aid membrane deformation. This is the case for a peptide known as Cholera Toxin B-subunit (CTxB), which can induce phase separation from uniformly mixed artificial liposomes upon deformation (Sorre et al., 2009). CTxB can bind 5 molecules of GM1 sphingolipid (a kind of ganglioside), therefore lowering the entropic

cost to transiently form L_0 phase from liposomes close to phase transition. These promising observations are likely to happen *in vivo* as evidences suggest with shiga toxin induced membrane invaginations (Römer et al., 2007).

As exposed in the lines before, the combination of molecular biology and soft matter physics has proved to be extremely fruitful for understanding the link between lipid shape and physical properties of biological membranes. The challenge that remains ahead is to find which of these observations are the tools used by proteins to sense and tune the physical state of membranes.

Tools to sense and modify membrane composition.

Cells use proteins as tools to sense the local lipid composition of a membrane. These tools can sense the characteristics discussed before, such as packing defects, membrane order or shape. These proteins generally participate in membrane deformation events, some can actively deform membranes, other can sense curvature and perhaps some could locally generate conical lipids to facilitate membrane deformation.

Amphipathic Lipid-Packing Sensing motifs (ALPS) help proteins to find packing defects on membranes. These motifs have been found in proteins functionally related to the nuclear envelope and early secretory pathway (Bigay and Antonny, 2012). The motif consists of bulky hydrophobic residues which is unfolded in the cytosol and folds as an amphipathic helix when inserted in membranes. ALPS insertion is membrane favoured by membrane curvature and conical lipids (Bigay et al., 2005). Molecular dynamic simulations and circular dichroism spectroscopy have shown that bulky residues of ALPS motif gets inserted into regions with large packing defects, allowing the protein to explore the surface of the membrane (Vanni et al., 2013). One of the main conclusions of these studies is that ALPS motifs are sensitive to the abundance of large hydrophobic mismatches rather than to the localization of specific lipids or curvature itself. As discussed before, conical lipids can generate large packing defects (Vamparys et al., 2013) even in flat bilayers. Curvature would also increase the abundance of these packing defects, therefore acting as a bait for proteins with ALPS motifs.

More evidence points in the direction that membrane binding proteins require specific membrane parameters to change the shape of a bilayer into a vesicle. Experiments using GUVs can be used to recreate the recruitment and scaffolding of COPI coats onto lipid bilayers (Manneville et al., 2008). Using ternary mixtures to form GUVs with visible phase separation, COPI binds exclusively to those regions of the membrane exhibiting L_d phases. Furthermore, COPI machinery is only able to efficiently deform the surface of GUVs under low tension circumstances. Strong tubulation from L_d phase is only observed at low tension, meaning that Arf1 and COPI coats scaffold and deform membranes preferentially under

these circumstances. Although phase separation in artificial liposomes may not be directly extrapolable to *in vivo* circumstances, it gives a clear picture that vesicle coat formation is an interplay between curvature generating coats and modulation of membrane properties. Regarding these results one can argue that there is no need for conical lipids to have a favourable bilayer for vesicle formation, since L_d and low tension can be achieved without them. Indeed, conical lipid shapes may not be essential *per se*, but they favour L_d phases, helping to carry out vesicle formation events *in vivo*.

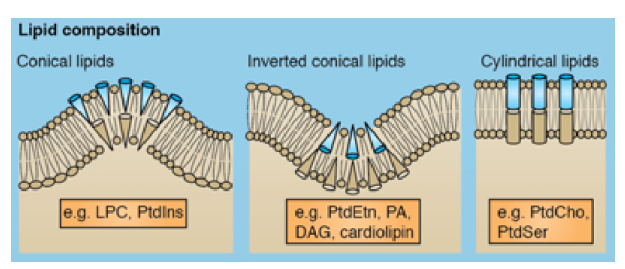


Figure 3. Modified from (McMahon and Boucrot, 2015). Spontaneous curvature of bilayers caused by lipid shape. The average shape of the lipids composing a bilayer can cause its spontaneous deformation.

While searching for low free energy states, contiguous lipids with different structural shape may increase lateral pressure between acyl chains inside the bilayer, therefore causing an increase of local energy. This state is often described as geometrically frustrated system, where none of its elements is in its lower energy state. This energy gain can be relaxed by curving the membrane, allowing for a better imbrication of lipids shapes (Figure 3). However, the final curvature obtained will be the best compromise for all lipids, but not the best curvature for a single species (Seddon and Templer, 1995). For example, conical lipids present in the outer leaflet will promote positive curvature, whereas in the other leaflet will promote negative curvature. Thus, changes in acyl chain number and length, which dramatically affect the lipid shape is thought to promote spontaneous curvature. Conical lipids can be generated through membrane remodeling by enzymes that can modify the structure of previously cylindric lipids. Some of these enzymes are cytosolic, others are transmembrane or anchored to glycosylphosphatidylinositol (GPI). Their activity is limited to just one leaflet of the bilayer, modifying the lipids around them. A specific set of enzymes can change the structure of lipids by acylation or deacylation (Lands, 2000) (figure 4). Phospholipases can remove acyl-chains from positions sn-1 or sn-2, generating lysophospholipid species and free fatty acids (FFA).

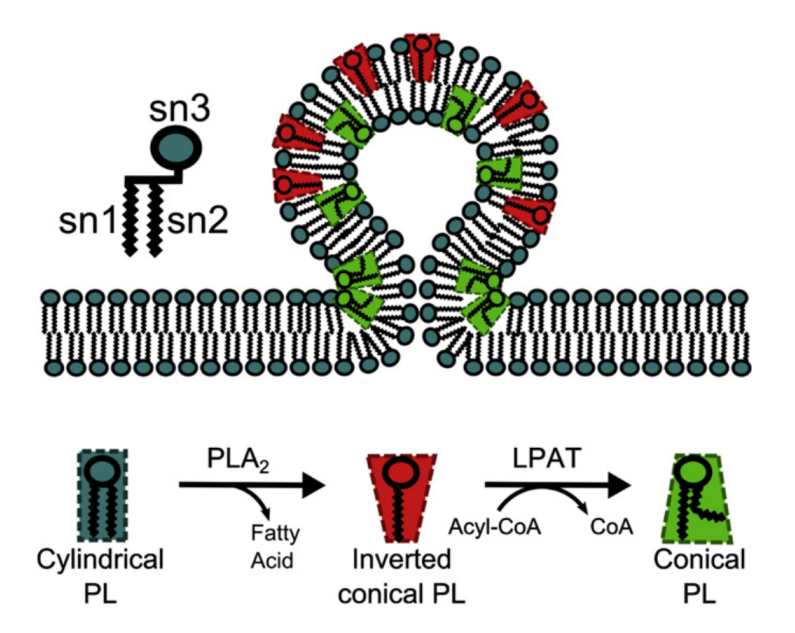


Figure 4. Reproduced from (Ha et al., 2012) A representation of Lands cycle in the context of transport vesicle formation. Phospholipases would hydrolyze an acyl chain from a cylindrical phospholipase, thus generating a conical lysophospholipid that could potentially aid coats to generate positive curvature or negative curvature. A subsequent reacylation of these lysophospholipids could lead to the formation of conical phospholipids species, which could aid in the generation of negative curvature or changing the order of the membrane.

The counterpart of phospholipases are lysophospholipid acyltransferases (LPAT), capable of re-acylating lysophospholipids, with same or different type of acyl-chain. Another type of phospholipase (named D or C) are those that can hydrolyze the headgroup of a glycerophospholipid, releasing PA or diacylglycerol (DAG), respectively, and a free polar section, with or without phosphate. While both PA and DAG could help to make membranes more deformable (Kooijman et al., 2005), the free polar group can also have great implications in signaling cascades, such as the case of phosphoinositides (Balla, 2013). Over the past decades, phospholipases and acyltransferases have been related to the secretory pathway in many ways, however the evidence was difficult to reconcile with the well documented mechanism stemming from the understanding of the minimal machineries of vesicular transport. A long-standing question is whether conical lipids could have an active role in membrane deformation mediated by coatomer, and if so, how would this be mediated. Early reports showed that Arf1, a small GTPase critical for COPI budding at Golgi apparatus, stimulated phospholipase D activity, suggesting a possible role of PA in COPI vesicle generation (Brown et al., 1993). Similar results were found for Sar1, a small GTPase coordinating COPII vesicle formation at the ER (Pathre et al., 2003). This suggest that small GTPases, which are known to induce curvature and packing defects, could serve as a positive regulator of conical lipids generation, perhaps increasing the abundance and size of packing defects. Other evidence suggests that lysophosphatidic acid acyltransferase 3 (LPAAT3) plays a role in COPI vesicle formation (Schmidt and Brown, 2009). The roles of PA in COPI and COPII vesicle formation is not clear yet. One possibility is that their negative charge would help to attract coat proteins to domains where membrane deformation is taking place. Another possibility is that the intrinsic conical shape of PA could participate in making the membrane more accessible to coat proteins through introducing packing defects.

There are a lot of evidence linking lysophospholipids to membrane deformation events along the secretory pathway (Ha et al., 2012). Early studies showed phospholipase A_2 (PLA₂) to be dependent on "bilayer microheterogeneity" for optimal hydrolytic activity of phospholipids. This was deduced by the slow activity of PLA₂ when hydrolyzing a gel phase of PC. After a lag period, a burst of PLA₂ activity can be assessed in liposomes or supported bilayers (Hønger et al., 1996; Nielsen et al., 1999). Further observations with atomic force microscopy (AFM) showed that there was no lag time when holes were generated with the AFM on a supported bilayer of PC (Grandbois et al., 1998). The enzymes started to hydrolyze the lipids from the edges of the holes, initially creating channels that disappeared with time, probably due to the change of state of the bilayer from gel state to L_o or L_d , where PLA₂ could easily access the bilayer at any point. These experiments suggest that membrane curvature and/or packing defects could serve as bait to attract membrane remodeling enzymes. This is not limited to phospholipases: there are reports that show a dependence of sphingomyelinases on packing defects (Ruiz-Argüello et al., 2002), which suggest similar features for membrane remodeling enzymes.

This has been seen by many as potential way to modify the shape of membranes by changing its spontaneous curvature. Most likely membrane remodeling would facilitate local lipid heterogeneities or increase their abundance in regions of membrane deformation, aiding coats to penetrate into the bilayer and perhaps changing elastic properties of membranes such as bending rigidity. Precise mechanisms to explain how lipid remodeling could work in conjunction with membrane deformation machineries still needs to be fully explored. Future work assessing *in vivo* physical parameters of membranes will draw more light on the precise role lipids may have not only in membrane deformation, but also lipid and protein sorting along the secretory pathway.

Membrane deformation in vesicle formation.

Despite cellular organelles are closed membrane structures, they are not isolated entities at all. Intense vesicular traffic transport proteins and lipids from one organelle to another, allowing the organelles to remain independent and at the same time exchange materials (figure 5). Interestingly, not all organelles are part of this vesicular transport, which

evidences the existence of parallel non-vesicular transport connecting these organelles to the rest of the cell.

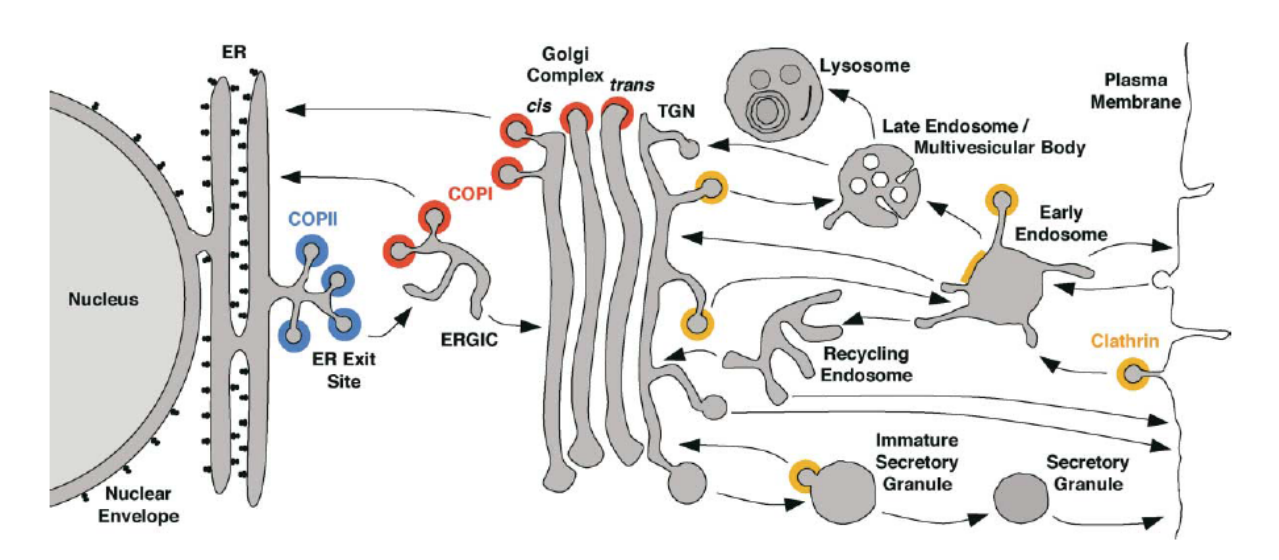


Figure 5. Reproduced from (Bonifacino and Glick, 2004). Intracellular transport pathways, indicated with arrows among the different organelles. Colors scheme indicate the location locations of COPII (blue), COPI (red), and clathrin (orange). The existence of other coats or coat-like complexes have been documented but are not shown in this figure.

The ground principles of vesicular transport are similar regardless of the organelle of origin or target destination (Bonifacino and Glick, 2004). The bilayer from a donor compartment is deformed into an extremely curved bilayer (varying from 70 to 100 nm in diameter) which contains the proteins that will be transported, named as cargo. A last and critical step required is the scission of the nascent vesicle from the donor compartment to finally release a free vesicle in the cytoplasm. These membrane shuttles will later fuse with the target organelle, delivering the protein and lipid content.

Both membrane deformation and cargo selection are mediated by multiple proteins that assemble over the surface of the organelle, acting as coats. These coats are recruited from the cytosol and bind to specific membranes, generally recruited by other proteins. Furthermore, once the vesicles have pinched off from the donor organelle, the coats disassemble from the vesicle and can be recycled for another round of vesicle formation.

Interestingly, eukaryotic cells have developed several different systems to generate vesicles. Clathrin complex were the first coats to be identified (Pearse, 1976; Roth and Porter, 1964). Their function is restricted from post Golgi compartments to the plasma membrane, with critical functions in extra cellular uptakes and plasma membrane protein internalization.

COPII mediates the transport of proteins from the ER to the Golgi apparatus or trans-Golgi network (TGN), and is the starting point of the secretory pathway (Miller and Schekman, 2013a). Retrograde transport and transport within Golgi stacks is mediated by a latter coat complex known as COPI (Popoff et al., 2011).

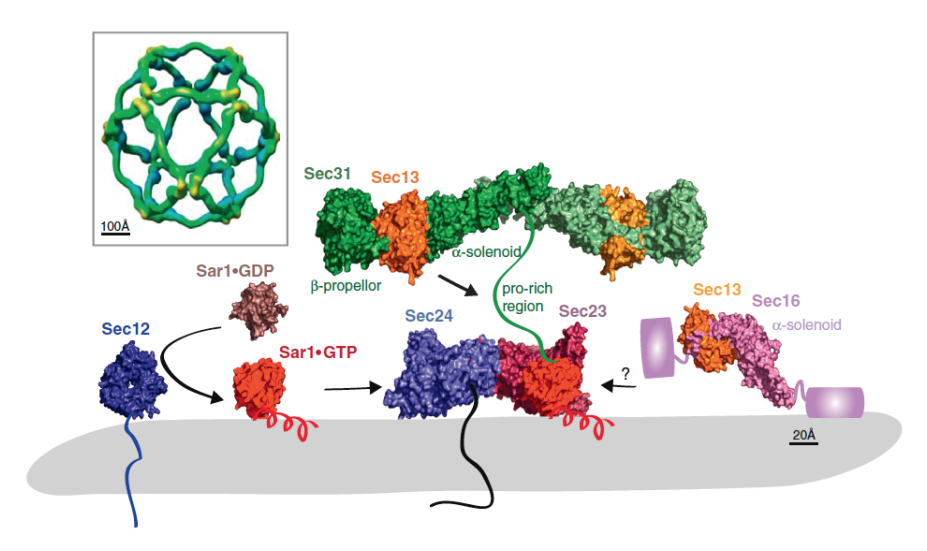


Figure 6. Reproduced from (Miller and Schekman, 2013a). Structure and assembly of the COPII coat. Sec12 favours the exchange of GDP for GTP on Sar1, which exposes an N-terminal amphipathic alpha-helix and bind to ER surface. This recruits Sec23/24 heterodimer. Sec24 provides interacts physically with sorting signals on transmembrane cargo. Sar1 together with Sec23/24 forms a pre-budding complex that recruits Sec13/31 heterotetramer. Furthermore, Sec13/31 scaffolds into a polyhedral cage driving at least in part membrane deformation into a positively curved structure and vesicle scission. Sec23 and Sec31 are GAP proteins for Sar1, regulating GTP hydrolysis via a proline-rich domain. Sec16 is a peripheral membrane bound protein that binds to Sec13 and modulates GTPase activity by inhibiting Sec31 GAP activity. Sec16 participates in ERES formation, although is not well understood.

Of special interest to the work described in this thesis is COPII complex. The minimal machinery of COPII coat is composed by five cytoplasmic proteins that assemble sequentially on the ER surface (Barlowe et al., 1994). Coat assembly is initiated by transmembrane protein Sec12, which acts as a GTP exchange factor (GEF) on Sar1 GTPase. The latter inserts a hydrophobic alpha-helix on the outer leaflet of the ER and once there recruits Sec23/24 heterodimer and finally Sec13/31 heterotetramer (Figure 6) (Miller and Schekman, 2013b). Cargo proteins are recognized and packaged into vesicles by Sec23/24 proteins and their homologs (Manzano-Lopez et al., 2015), followed by Sec13/31 polymerization over Sec23/24 subcomplexes thus generating membrane deformation into an extremely curved vesicle (Copic et al., 2012). The process of COPII vesicle formation define a specific subdomains of the ER known as ER exit sites (ERES), where cargo and COPII proteins meet to form vesicles (Orci et al., 1991). Interestingly, the distribution and duration of the ERES changes among different organisms (Montegna et al., 2012). The assembly of

COPII is in part self regulated by the coat, as Sec23 and Sec31 GTPase activating proteins (GAP) on Sar1 (Antonny et al., 2001). Regulation of the coat is also regulated by proteins that accessory proteins that stand nearby vesicle formation. Sec16 participates in this regulation by modulating Sec31 GAP activity.

Although the current knowledge regarding COPII assembly and cargo recognition has led to a clear picture of the principles of this system, much more is what is not understood. The precise mechanism on how the ERES are established is yet to be clarified. In yeast S. cerevisiae, ERES are transient structures with a limited lifetime of minutes (Shindiapina and Barlowe, 2010), while in yeast Pichia pastoris and animal cells ERES are permanent structures, nearby Golgi stacks. In S. cerevisiae, ERES are dependent on Sec12 and Sec16. The first is homogeneously distributed through the ER while the latter is localized at the ERES (Okamoto et al., 2012). Interestingly, ERES display a positive shallow curvature compared to the regions around. How this curvature is generated is not well understood, could be generated by COPII machinery itself. Conical lipids could help or mediate this binding generating packing defects and/or lowering bending rigidity. In fact, conical lipids have been linked functionally with COPII and ERES in many ways. Mammalian PLA-like protein p125 interacts in an ill defined way with Sec13/31, which is part of COPII machinery and p125 localizes at the ERES (Ong et al., 2010a; Shimoi et al., 2005a). This evidence suggests the presence of lysophospholipids at the ERES. This fits well with early in vitro COPII reconstitutions, where lysophospholipids were found to enhance Sar1 binding to liposomes (Matsuoka et al., 1998), perhaps by inducing local packing defects suitable for initial states of coat binding. One could speculate that COPII, as well as COPI, could also require L_d and low membrane rigidity to deform a membrane full of cargo proteins. If this is true, conical lipids would promote L_d and therefore binding of COPII. Furthermore, COPII coats are sensitive to cargo accumulation as mutations affecting cargo accumulation can alleviate deleterious phenotype of sec13 mutants (Copic et al., 2012; Derganc et al., 2013). If COPII membrane deformation is dependent on cargo accumulation, it is guite likely that lipid composition of the membrane could play a role as well.

The idea behind this thesis is that certain lipid types are required for an efficient COPII vesicle formation. I hypothesized that ERES may have specific lipid composition that will facilitate extreme deformations by lowering the energetic requirements to generate such extreme geometries. Having that lipids with conical shapes have been related before to vesicle formation processes, I propose that lipid species with conical structures are found and have a role in COPII vesicle formations. The work described in the following chapters give evidences that lysophosphoinositol could be directly linked to COPII biogenesis, probably due to the extreme conical shape of this lipid type.

Antonny, B., Madden, D., Hamamoto, S., Orci, L., and Schekman, R. (2001). Dynamics of the COPII coat with GTP and stable analogues. Nat. Cell Biol. 3, 531–537.

Balla, T. (2013). Phosphoinositides: tiny lipids with giant impact on cell regulation. Physiol. Rev. 93, 1019–1137.

Barlowe, C., Orci, L., Yeung, T., Hosobuchi, M., Hamamoto, S., Salama, N., Rexach, M.F., Ravazzola, M., Amherdt, M., and Schekman, R. (1994). COPII: a membrane coat formed by Sec proteins that drive vesicle budding from the endoplasmic reticulum. Cell 77, 895–907.

Baumgart, T., Hess, S.T., and Webb, W.W. (2003). Imaging coexisting fluid domains in biomembrane models coupling curvature and line tension. Nature *425*, 821–824.

Bigay, J., and Antonny, B. (2012). Curvature, lipid packing, and electrostatics of membrane organelles: defining cellular territories in determining specificity. Dev. Cell 23, 886–895.

Bigay, J., Joëlle, B., Jean-François, C., Guillaume, D., Bruno, M., and Bruno, A. (2005). ArfGAP1 responds to membrane curvature through the folding of a lipid packing sensor motif. EMBO J. *24*, 2244–2253.

Bonifacino, J.S., and Glick, B.S. (2004). The mechanisms of vesicle budding and fusion. Cell *116*, 153–166.

Brown, H.A., Gutowski, S., Moomaw, C.R., Slaughter, C., and Sternweis, P.C. (1993). ADPribosylation factor, a small GTP-dependent regulatory protein, stimulates phospholipase D activity. Cell *75*, 1137–1144.

Callan-Jones, A., Sorre, B., and Bassereau, P. (2011a). Curvature-driven lipid sorting in biomembranes. Cold Spring Harb. Perspect. Biol. 3.

Callan-Jones, A., Sorre, B., and Bassereau, P. (2011b). Curvature-driven lipid sorting in biomembranes. Cold Spring Harb. Perspect. Biol. 3.

Copic, A., Latham, C.F., Horlbeck, M.A., D'Arcangelo, J.G., and Miller, E.A. (2012). ER cargo properties specify a requirement for COPII coat rigidity mediated by Sec13p. Science 335, 1359–1362.

Dennis, E.A., Deems, R.A., Harkewicz, R., Quehenberger, O., Brown, H.A., Milne, S.B., Myers, D.S., Glass, C.K., Hardiman, G., Reichart, D., et al. (2010). A mouse macrophage lipidome. J. Biol. Chem. *285*, 39976–39985.

Derganc, J., Antonny, B., and Copič, A. (2013). Membrane bending: the power of protein imbalance. Trends Biochem. Sci. 38, 576–584.

Dietrich, C., Bagatolli, L.A., Volovyk, Z.N., Thompson, N.L., Levi, M., Jacobson, K., and Gratton, E. (2001). Lipid rafts reconstituted in model membranes. Biophys. J. 80, 1417–1428.

Dreier, L., and Rapoport, T.A. (2000). In vitro formation of the endoplasmic reticulum occurs independently of microtubules by a controlled fusion reaction. J. Cell Biol. *148*, 883–898.

Evans, E., Evan., E., and David., N. (1987). Physical properties of surfactant bilayer membranes: thermal transitions, elasticity, rigidity, cohesion and colloidal interactions. J. Phys. Chem. *91*, 4219–4228.

Frisz, J.F., Klitzing, H.A., Lou, K., Hutcheon, I.D., Weber, P.K., Zimmerberg, J., and Kraft, M.L. (2013). Sphingolipid domains in the plasma membranes of fibroblasts are not enriched with cholesterol. J. Biol. Chem. 288, 16855–16861.

Grandbois, M., Michel, G., Hauke, C.-S., and Hermann, G. (1998). Atomic Force Microscope Imaging of Phospholipid Bilayer Degradation by Phospholipase A2. Biophys. J. *74*, 2398–2404.

Guan, X.L., Souza, C.M., Pichler, H., Dewhurst, G., Schaad, O., Kajiwara, K., Wakabayashi, H., Ivanova, T., Castillon, G.A., Piccolis, M., et al. (2009). Functional interactions between sphingolipids and sterols in biological membranes regulating cell physiology. Mol. Biol. Cell 20, 2083–2095.

Ha, K.D., Clarke, B.A., and Brown, W.J. (2012). Regulation of the Golgi complex by phospholipid remodeling enzymes. Biochim. Biophys. Acta *1821*, 1078–1088.

Hao, M., Mukherjee, S., and Maxfield, F.R. (2001). Cholesterol depletion induces large scale domain segregation in living cell membranes. Proc. Natl. Acad. Sci. U. S. A. 98, 13072–13077.

Holthuis, J.C.M., and Menon, A.K. (2014). Lipid landscapes and pipelines in membrane homeostasis. Nature *510*, 48–57.

Hønger, T., Jørgensen, K., Biltonen, R.L., and Mouritsen, O.G. (1996). Systematic relationship between phospholipase A2 activity and dynamic lipid bilayer microheterogeneity. Biochemistry *35*, 9003–9006.

Ingólfsson, H.I., Melo, M.N., van Eerden, F.J., Arnarez, C., Lopez, C.A., Wassenaar, T.A., Periole, X., de Vries, A.H., Tieleman, D.P., and Marrink, S.J. (2014). Lipid organization of the plasma membrane. J. Am. Chem. Soc. *136*, 14554–14559.

Ipsen, J.H., Karlström, G., Mouritsen, O.G., Wennerström, H., and Zuckermann, M.J. (1987). Phase equilibria in the phosphatidylcholine-cholesterol system. Biochim. Biophys. Acta *905*, 162–172.

Janmey, P.A., and Kinnunen, P.K.J. (2006). Biophysical properties of lipids and dynamic membranes. Trends Cell Biol. *16*, 538–546.

Klemm, R.W., Ejsing, C.S., Surma, M.A., Kaiser, H.-J., Gerl, M.J., Sampaio, J.L., de Robillard, Q., Ferguson, C., Proszynski, T.J., Shevchenko, A., et al. (2009). Segregation of sphingolipids and sterols during formation of secretory vesicles at the trans-Golgi network. J. Cell Biol. *185*, 601–612.

Kooijman, E.E., Vladimir, C., Fuller, N.L., Kozlov, M.M., de Kruijff, B., Burger, K.N.J., and Rand, P.R. (2005). Spontaneous Curvature of Phosphatidic Acid and Lysophosphatidic Acid †. Biochemistry *44*, 2097–2102.

Lands, W.E.M. (2000). Stories about acyl chains. Biochimica et Biophysica Acta (BBA) - Molecular and Cell Biology of Lipids *1483*, 1–14.

Lewis, B.A., and Engelman, D.M. (1983). Lipid bilayer thickness varies linearly with acyl chain length in fluid phosphatidylcholine vesicles. J. Mol. Biol. *166*, 211–217.

Luzzati, V., Tardieu, A., and Gulik-Krzywicki, T. (1968). Polymorphism of lipids. Nature *217*, 1028–1030.

Manneville, J.-B., Casella, J.-F., Ambroggio, E., Gounon, P., Bertherat, J., Bassereau, P.,

Cartaud, J., Antonny, B., and Goud, B. (2008). COPI coat assembly occurs on liquid-disordered domains and the associated membrane deformations are limited by membrane tension. Proc. Natl. Acad. Sci. U. S. A. 105, 16946–16951.

Manzano-Lopez, J., Javier, M.-L., Perez-Linero, A.M., Auxiliadora, A.-R., Martin, M.E., Tatsuki, O., Silva, D.V., Seeberger, P.H., Howard, R., Kouichi, F., et al. (2015). COPII Coat Composition Is Actively Regulated by Luminal Cargo Maturation. Curr. Biol. *25*, 152–162.

Matsuoka, K., Orci, L., Amherdt, M., Bednarek, S.Y., Hamamoto, S., Schekman, R., and Yeung, T. (1998). COPII-coated vesicle formation reconstituted with purified coat proteins and chemically defined liposomes. Cell *93*, 263–275.

McMahon, H.T., and Boucrot, E. (2015). Membrane curvature at a glance. J. Cell Sci. *128*, 1065–1070.

McMahon, H.T., and Gallop, J.L. (2005). Membrane curvature and mechanisms of dynamic cell membrane remodelling. Nature *438*, 590–596.

van Meer, G. (2011). Dynamic transbilayer lipid asymmetry. Cold Spring Harb. Perspect. Biol. 3.

Miller, E.A., and Schekman, R. (2013a). COPII - a flexible vesicle formation system. Curr. Opin. Cell Biol. *25*, 420–427.

Miller, E.A., and Schekman, R. (2013b). COPII - a flexible vesicle formation system. Curr. Opin. Cell Biol. *25*, 420–427.

Montegna, E.A., Bhave, M., Liu, Y., Bhattacharyya, D., and Glick, B.S. (2012). Sec12 binds to Sec16 at transitional ER sites. PLoS One 7, e31156.

Nielsen, L.K., Jens, R., Callisen, T.H., and Thomas, B. (1999). Lag-burst kinetics in phospholipase A2 hydrolysis of DPPC bilayers visualized by atomic force microscopy. Biochimica et Biophysica Acta (BBA) - Biomembranes *1420*, 266–271.

Okamoto, M., Kurokawa, K., Matsuura-Tokita, K., Saito, C., Hirata, R., and Nakano, A. (2012). High-curvature domains of the ER are important for the organization of ER exit sites in Saccharomyces cerevisiae. J. Cell Sci. *125*, 3412–3420.

Ong, Y.S., Tang, B.L., Loo, L.S., and Hong, W. (2010a). p125A exists as part of the mammalian Sec13/Sec31 COPII subcomplex to facilitate ER-Golgi transport. J. Cell Biol. 190, 331–345.

Ong, Y.S., Tang, B.L., Loo, L.S., and Hong, W. (2010b). p125A exists as part of the mammalian Sec13/Sec31 COPII subcomplex to facilitate ER-Golgi transport. J. Cell Biol. 190, 331–345.

Orci, L., Ravazzola, M., Meda, P., Holcomb, C., Moore, H.P., Hicke, L., and Schekman, R. (1991). Mammalian Sec23p homologue is restricted to the endoplasmic reticulum transitional cytoplasm. Proc. Natl. Acad. Sci. U. S. A. 88, 8611–8615.

Pathre, P., Shome, K., Blumental-Perry, A., Bielli, A., Haney, C.J., Alber, S., Watkins, S.C., Romero, G., and Aridor, M. (2003). Activation of phospholipase D by the small GTPase Sar1p is required to support COPII assembly and ER export. EMBO J. 22, 4059–4069.

Patton, J.L., and Lester, R.L. (1991). The phosphoinositol sphingolipids of Saccharomyces cerevisiae are highly localized in the plasma membrane. J. Bacteriol. *173*, 3101–3108.

Pearse, B.M. (1976). Clathrin: a unique protein associated with intracellular transfer of membrane by coated vesicles. Proceedings of the National Academy of Sciences 73, 1255–1259.

Pietiläinen, K.H., Róg, T., Seppänen-Laakso, T., Virtue, S., Gopalacharyulu, P., Tang, J., Rodriguez-Cuenca, S., Maciejewski, A., Naukkarinen, J., Ruskeepää, A.-L., et al. (2011). Association of lipidome remodeling in the adipocyte membrane with acquired obesity in humans. PLoS Biol. 9, e1000623.

Popoff, V., Adolf, F., Brügger, B., and Wieland, F. (2011). COPI budding within the Golgi stack. Cold Spring Harb. Perspect. Biol. 3, a005231.

Römer, W., Berland, L., Chambon, V., Gaus, K., Windschiegl, B., Tenza, D., Aly, M.R.E., Fraisier, V., Florent, J.-C., Perrais, D., et al. (2007). Shiga toxin induces tubular membrane invaginations for its uptake into cells. Nature *450*, 670–675.

Roth, T.F., and Porter, K.R. (1964). YOLK PROTEIN UPTAKE IN THE OOCYTE OF THE MOSQUITO AEDES AEGYPTI. L. J. Cell Biol. 20, 313–332.

Roux, A., Cuvelier, D., Nassoy, P., Prost, J., Bassereau, P., and Goud, B. (2005). Role of curvature and phase transition in lipid sorting and fission of membrane tubules. EMBO J. *24*, 1537–1545.

Ruiz-Argüello, M.B., Veiga, M.P., Arrondo, J.L.R., Goñi, F.M., and Alonso, A. (2002). Sphingomyelinase cleavage of sphingomyelin in pure and mixed lipid membranes. Influence of the physical state of the sphingolipid. Chem. Phys. Lipids *114*, 11–20.

Saleem, M., Morlot, S., Hohendahl, A., Manzi, J., Lenz, M., and Roux, A. (2015). A balance between membrane elasticity and polymerization energy sets the shape of spherical clathrin coats. Nat. Commun. *6*, 6249.

Sampaio, J.L., Gerl, M.J., Klose, C., Ejsing, C.S., Beug, H., Simons, K., and Shevchenko, A. (2011). Membrane lipidome of an epithelial cell line. Proc. Natl. Acad. Sci. U. S. A. *108*, 1903–1907.

Schmidt, J.A., and Brown, W.J. (2009). Lysophosphatidic acid acyltransferase 3 regulates Golgi complex structure and function. J. Cell Biol. *186*, 211–218.

Schneiter, R., Brügger, B., Sandhoff, R., Zellnig, G., Leber, A., Lampl, M., Athenstaedt, K., Hrastnik, C., Eder, S., Daum, G., et al. (1999). Electrospray ionization tandem mass spectrometry (ESI-MS/MS) analysis of the lipid molecular species composition of yeast subcellular membranes reveals acyl chain-based sorting/remodeling of distinct molecular species en route to the plasma membrane. J. Cell Biol. *146*, 741–754.

Seddon, J.M., and Templer, R.H. (1995). Polymorphism of Lipid-Water Systems. In Handbook of Biological Physics, pp. 97–160.

Shevchenko, A., and Simons, K. (2010). Lipidomics: coming to grips with lipid diversity. Nat. Rev. Mol. Cell Biol. *11*, 593–598.

Shibata, Y., Voeltz, G.K., and Rapoport, T.A. (2006). Rough sheets and smooth tubules. Cell *126*, 435–439.

Shimoi, W., Ezawa, I., Nakamoto, K., Uesaki, S., Gabreski, G., Aridor, M., Yamamoto, A., Nagahama, M., Tagaya, M., and Tani, K. (2005a). p125 is localized in endoplasmic reticulum exit sites and involved in their organization. J. Biol. Chem. *280*, 10141–10148.

Shimoi, W., Ezawa, I., Nakamoto, K., Uesaki, S., Gabreski, G., Aridor, M., Yamamoto, A., Nagahama, M., Tagaya, M., and Tani, K. (2005b). p125 is localized in endoplasmic reticulum exit sites and involved in their organization. J. Biol. Chem. 280, 10141–10148.

Shindiapina, P., and Barlowe, C. (2010). Requirements for transitional endoplasmic reticulum site structure and function in Saccharomyces cerevisiae. Mol. Biol. Cell *21*, 1530–1545.

Singer, S.J., and Nicolson, G.L. (1972). The Fluid Mosaic Model of the Structure of Cell Membranes. Science *175*, 720–731.

Sorre, B., Callan-Jones, A., Manneville, J.-B., Nassoy, P., Joanny, J.-F., Prost, J., Goud, B., and Bassereau, P. (2009). Curvature-driven lipid sorting needs proximity to a demixing point and is aided by proteins. Proc. Natl. Acad. Sci. U. S. A. *106*, 5622–5626.

Tenchov, B., Boris, T., and Rumiana, K. (2012). Cubic phases in membrane lipids. Eur. Biophys. J. *41*, 841–850.

Vamparys, L., Gautier, R., Vanni, S., Bennett, W.F.D., Tieleman, D.P., Antonny, B., Etchebest, C., and Fuchs, P.F.J. (2013). Conical lipids in flat bilayers induce packing defects similar to that induced by positive curvature. Biophys. J. *104*, 585–593.

Vanni, S., Stefano, V., Lydie, V., Romain, G., Guillaume, D., Catherine, E., Fuchs, P.F.J., and Bruno, A. (2013). Amphipathic Lipid Packing Sensor Motifs: Probing Bilayer Defects with Hydrophobic Residues. Biophys. J. *104*, 575–584.

Chapter II:

Defects in COPII vesicle formation are rescued by phospholipase overexpression.

The endoplasmic reticulum (ER) serves as a platform for synthesis of secretory and transmembrane proteins, as well being the site of synthesis of most of cellular lipids. The ER is as well the origin of the secretory pathway as the source of vesicular transport of proteins and lipids to the Golgi apparatus (Barlowe and Miller, 2013). This transport is mediated by COPII coats, a protein complex that sequentially assembles over the ER surface; Sar1 GTPase recruits Sec23/24 heterodimer and finally Sec13/31 heterotetramer (Miller and Schekman, 2013). As described previously in chapter I, the recruitment of COPII proteins is initiated by Sec12, a transmembrane ER resident protein that promotes the exchange of GDP by GTP on Sar1 (Barlowe and Schekman, 1993). Cargo proteins and COPII machinery localize at discrete areas of ER membrane, defined as ER exit sites (ERES). In Saccharomyces cerevisiae these ERES are dynamic structures that form and disappear constantly along the cortical and perinuclear ER (Montegna et al., 2012). Sec12 plays a major role in ERES organization as evidenced by observation of the thermosensitive mutant allele sec12-4. When sec12-4 mutant yeast are incubated at non permissive temperature ($\geq 30^{\circ}$ C), ERES are disorganized and secretion is blocked, which finally leads to cell death (Castillon et al., 2009; Nakano et al., 1988; Shindiapina and Barlowe, 2010). Screens have identified suppressors of the sec12-4 phenotype (Elrod-Erickson and Kaiser, 1996; Murakami et al., 1999) and more recently, a suppressors involved in lipid homeostasis have been identified by Funato and collaborators (Kajiwara et al., 2013). In the latter work, deletion of several Osh genes (OSH2, OSH3 and OSH4) in a sec12-4 mutant strain was found to suppress both the growth defects and the ERES phenotype of sec12-4. Since Osh proteins have been proposed to participate in intracellular lipid transport, the lipidome of the strain was analyzed by mass spectrometry in collaboration with between the Funato and Riezman labs. Strikingly, sec12-4 $osh2\Delta$ $osh4\Delta$ had almost no change of ceramides and sterols levels compared to wild type yeast. The most noticeable change was an increase in lysophospholipids (data not shown). Another strain generated from Funato and Riezman collaboration was the double mutant sec12-4 arv1Δ, which also suppressed sec12-4 growth phenotype. The lipidome of this double mutant had something in common with sec12-4 $osh2\Delta$ $osh4\Delta$, an enrichment in lysophospholipids. This striking coincidence suggested a participation of lysophospholipids in the process of secretion from the ER. Perhaps lysophospholipids could play a role in ERES formation and COPII vesicle formation. However, the link between lipid metabolism and membrane deformation is not obvious, especially because lysophospholipids are considered as a by-product in lipid remodeling and degradation, also they are not abundant lipids in the cell. A common thing among all lysophospholipid species is their rather conical structure, due to the relation between the steric diameter of their polar headgroups versus the steric diameter of their only acyl chain. Furthermore, the enzymes linked to the production of lysophospholipids in yeast are ER related phospholipases B, three GPI-anchored proteins PLB1, PLB2 and PLB3 and the transmembrane phospholipase NTE1. This suggest that lysophospholipid accumulation in the ER could mediate the suppression of sec12-4 phenotypes.

To better understand the role of lysophospholipids in COPII vesicle formation, genetic overexpression of different phospholipases has been performed to increase the accumulation of lysophospholipid species and study its effect on *sec12-4* mutant phenotypes.

Results.

To test whether lysophospholipids could rescue sec12-4 mutant growth defects, yeast phospholipases PLB1, PLB2 and PLB3 were cloned in high copy 2μ vectors and transformed in a sec12-4 mutant strain. The growth at different temperatures was tested in a spot assay for wild type yeast and different sec12-4 clones overexpressing each phospholipase B. Of all of the phospholipases, only PLB3 was found to rescue sec12-4 temperature sensitive growth defect (figure 1). Mutant strain sec12-4 was not able to grow at temperatures higher than 30°C, while PLB3 overexpression partially rescued growth at 33°C and weakly at 35°C. Under similar conditions, wild type strain growth was unaffected by temperature or PLB3 overexpression. Thus, PLB3 overexpression can alleviate sec12-4 growth defects, suggesting that lysophospholipids may participate in COPII vesicle formation.

Another phenotype of *sec12-4* mutant strains is an aberrant distribution of ERES in the cell. ERES are visible with fluorescent labels genetically fused to COPII machinery (Connerly et al., 2005).

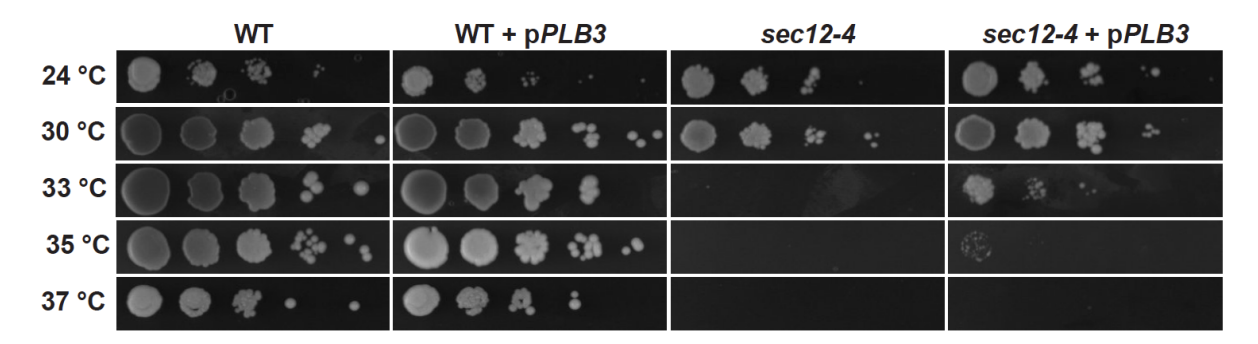


Figure 1. Overexpression of PLB3 rescues temperature sensitive growth defect of sec12-4 mutant. Fivefold serial dilution of 1 OD_{600} /ml of yeast culture were spotted onto YPD plates and were incubated at specified temperatures for 3 days.

Strains with mutant allele sec12-4 growing at restrictive temperatures accumulate COPII machinery in few large fluorescent puncta per cell (Castillon et al., 2009). Therefore, I hypothesized that PLB3 could rescue the accumulation of COPII proteins in aberrant puncta. To visualize the ERES on sec12-4 mutants, a yeast strain expressing sec12-4 mutation, wild type SEC13 and SEC13-GFP (random genomic insertion) was used (see materials and methods). Wild type yeasts were transformed with SEC13-mch plasmid as a control. Wild type strain as well as sec12-4 and sec12-4 overexpressing PLB3 strains were incubated at 24°C and the ERES were observed by epifluorescence. The number of ERES in sec12-4 mutant was similar with and without PLB3 overexpression, with an average number varying from 10 to 15 puncta per cell (figure 2). After 30 minutes of temperature shift to 30°C, mutant strain sec12-4 had an aberrant distribution of ERES, with one or two large puncta per cell instead of ERES distributed all along the cortical ER. Strikingly, this was not the case for sec12-4 overexpressing PLB3, whose ERES remained almost unchanged upon temperature shift (figure 2a). Nevertheless, some of these cells exhibited an intermediate phenotype, having both a large punctum and normally distributed ERES all over the cell, as can be seen from the quantification (figure 2b). Temperatures above 30°C increased the number of cells with large puncta in sec12-4 overexpressing PLB3 (data not shown). This shows that PLB3 overexpression can partially rescue the aberrant ERES distribution of sec12-4 at 30°C, but fails to rescue at higher temperature. Also, this suggests that lysophospholipids, may play a role in ERES organization and/or vesicle formation and overexpression of phospholipases may increase their amount and therefore their function, allowing the sec12-4 mutant to survive under more restrictive conditions.

PLB3 allows sec12-4 mutant to keep ERES distribution at otherwise non permissive temperature, perhaps the ERES of these strains are different in morphology to those of the sec12-4 mutant alone. To answer this question transmission electron microscopy was done on wild type, sec12-4 and sec12-4 overexpressing PLB3 strains. Cell cultures were incubated at 24°C and in early exponential phase were shifted to 33°C for 1 hour. At this point, cells were fixed with 2.5% glutaraldehyde for 1 hour. Negative stained images of wild type strains showed a clear cortical ER, juxtaposed to the plasma membrane, following the perimeter of the cell (figure 3). This was not the case for sec12-4 after 1 hour at 33°C. Cortical ER was not well defined or absent, perhaps present but scattered in the cytoplasm, where characteristic ER cisternae could sometimes be seen. Other structures such as small lightly stained structures resembling lipid bodies of 50-100 nm appeared in the cytoplasm (figure 3). Interestingly, sec12-4 overexpressing PLB3 showed almost no difference with wild type strain at 33°C (figure 3). Cortical ER was found in almost all cells observed, following the perimeter of the cell. A common feature with sec12-4 mutant was the presence of these small structures of 50-100 nm resembling lipid bodies. These results suggest the importance of ERES distribution and/or COPII vesicle formation for the structure of the ER. PLB3 overexpression could alter membrane composition and through this support efficient membrane deformation in situations where vesicle formation is compromised, as in the case of the sec12-4 mutant.

The opening question of this chapter is whether lysophospholipids could participate in COPII vesicle formation. As shown above, overexpression of a phospholipiase has a positive effect in sec12-4 mutant, which suggest a positive effect of lysophospholipids in COPII vesicle formation. However, if lysophospholipids are making a difference for sec12-4 mutant at nonpermissive conditions, we might be able to detect changes in the content of lysophospholipids in cells overexpressing PLB3. To examine this, the glycerophospholipid content of sec12-4 overexpressing PLB3 was measured by mass spectrometry. For this, cultures of wild type yeast, sec12-4 mutant and sec12-4 overexpressing PLB3 were grown at 24° C and 33° C in similar conditions in order to compare differences in glycerophospholipids.

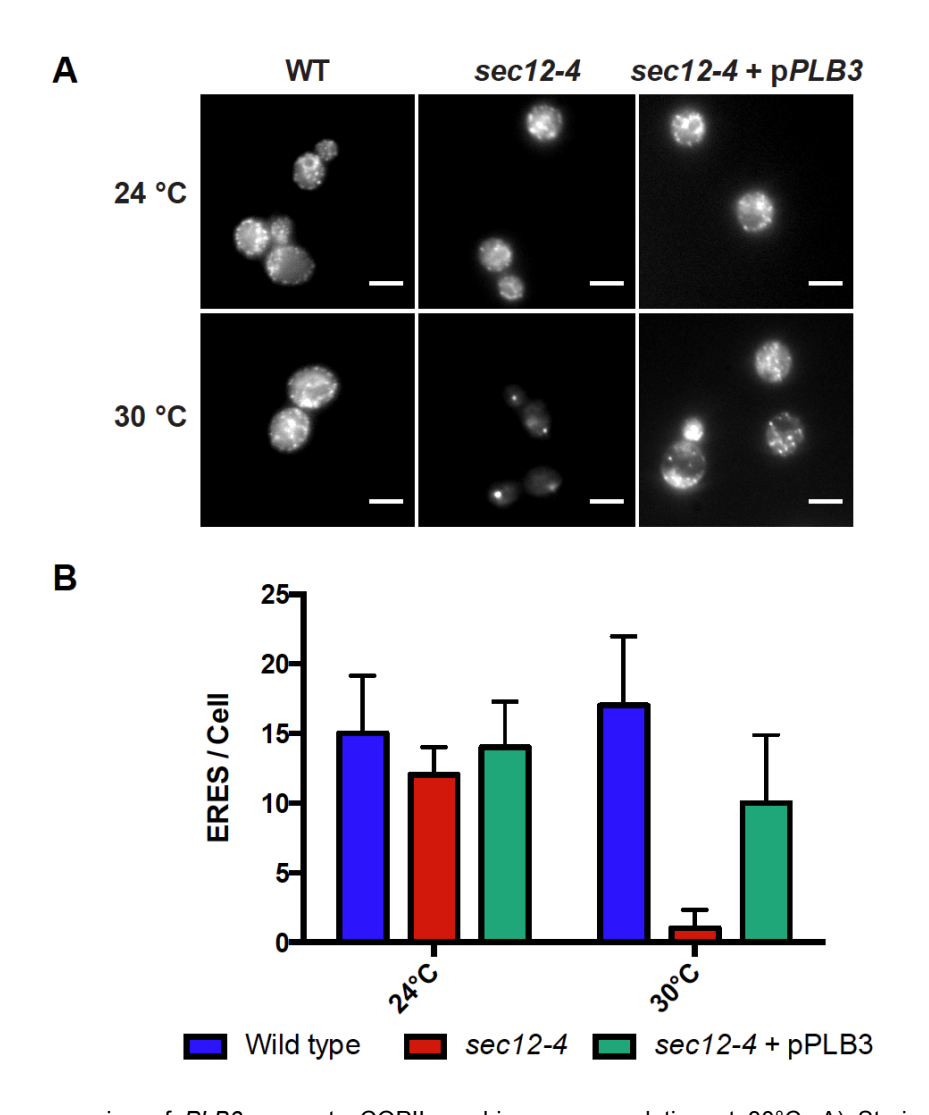


Figure 2. Overexpression of *PLB3* prevents COPII machinery accumulation at 30°C. A) Strains expressing sec13-GFP were used to visualize the ERES at 24°C and 30°C. Scale bar is 5 μ m. B) ERES per cell were counted and averaged for randomly chosen cells for each strain (WT n=10, sec12-4 n=13, sec12-4 +p*PLB3* n=13 at 24°C and n=16 at 30°C). Error bar represents standard deviation.

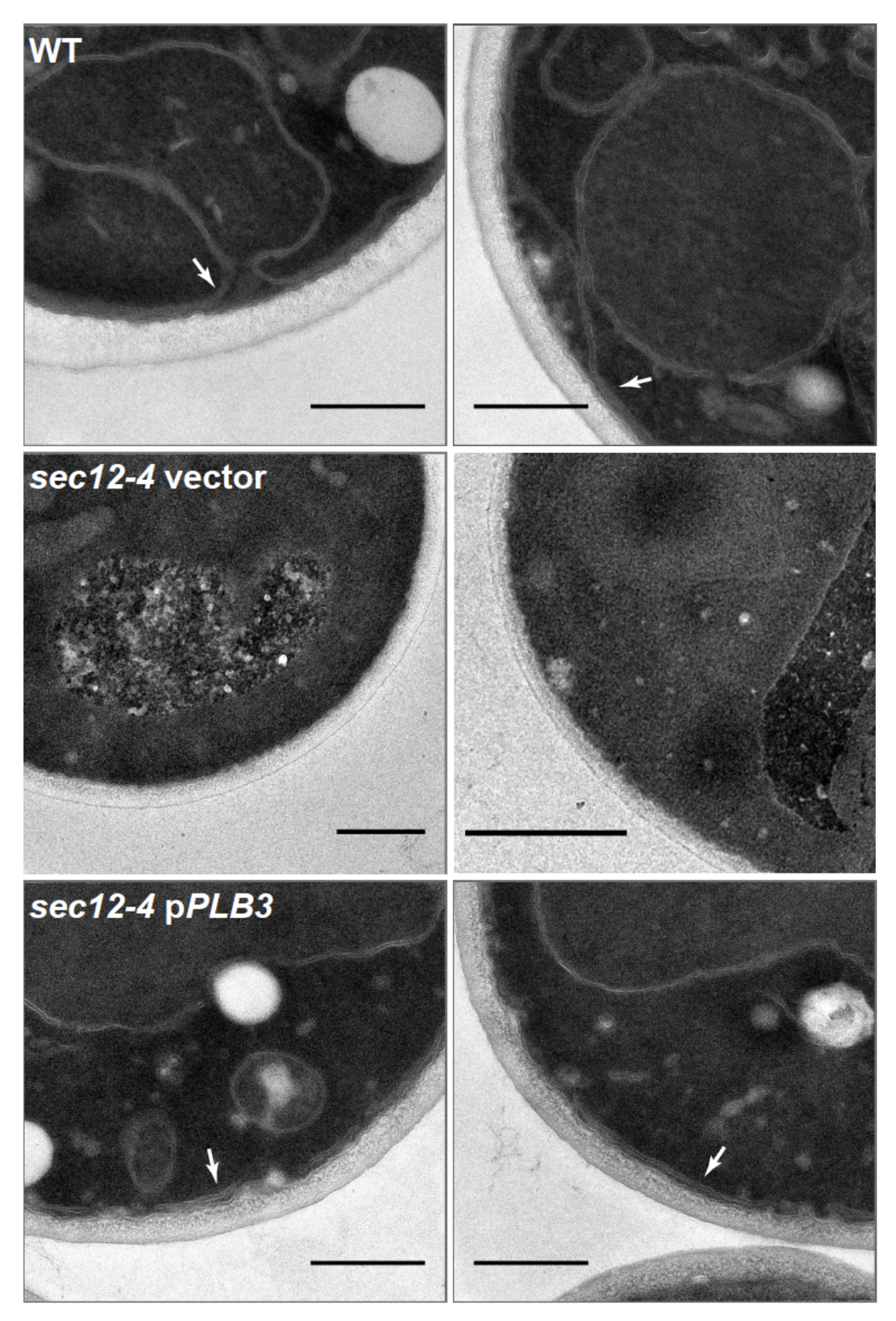


Figure 3. Mutant allele *sec12-4* seems to loose ER cortical organization at 33°C, while overexpression of *PLB3* corrects this defect. Arrows in WT and *sec12-4* p*PLB3* show regions where cortical ER can be observed. On the contrary, cortical ER is not visible in *sec12-4* mutant strain. Scale bar is 0.5μm.

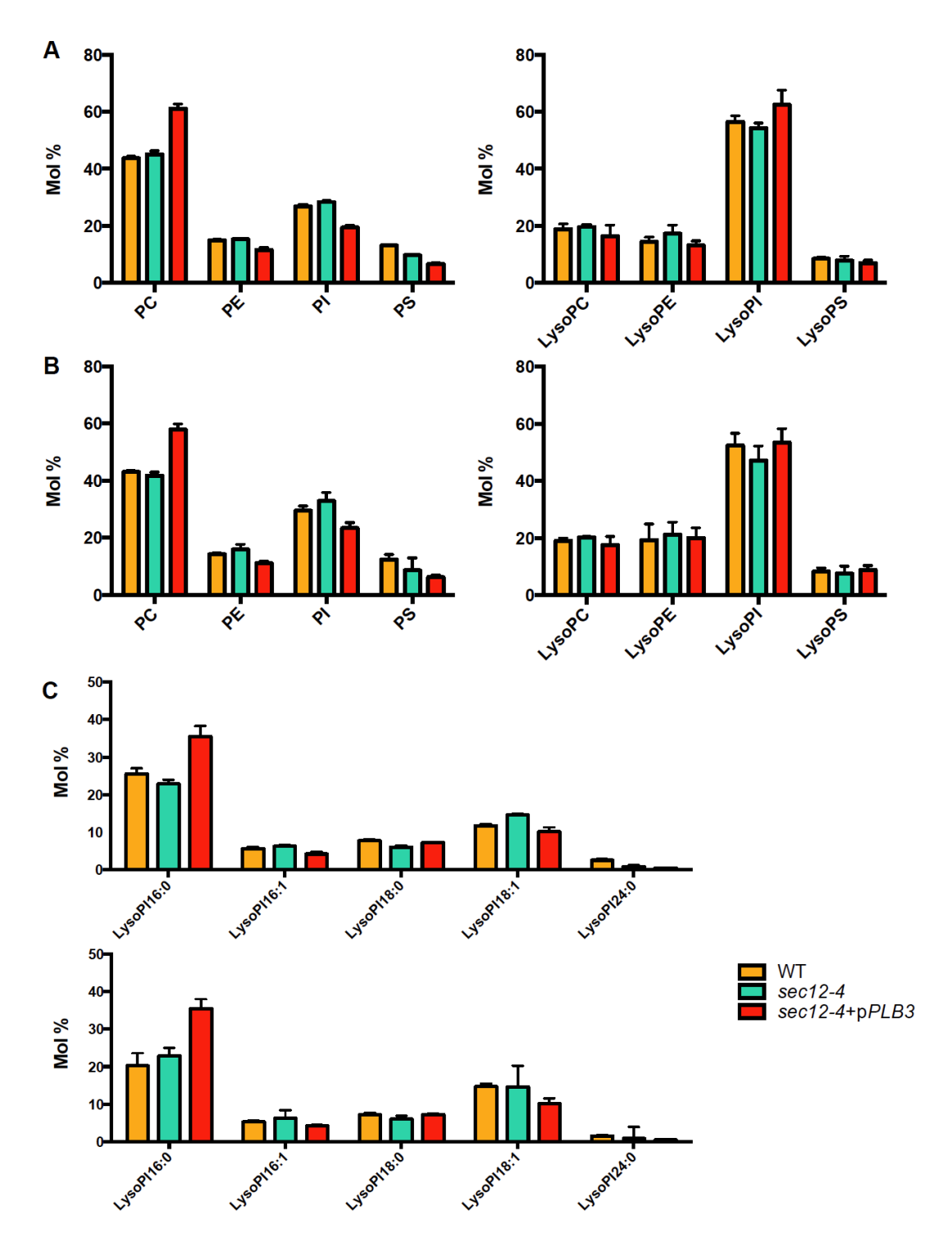


Figure 4. *PLB3* overexpression changes the lipid composition of *sec12-4* mutant. All strains were grown on selective media overnight at 24°C. At 0.5 OD₆₀₀/ml cells were collected and resuspended in YPD and each culture was split in two. One half continued growing at 24°C while the other half was placed at 33°C. Cells were collected when cultures reached 1 OD₆₀₀/ml and processed for lipid extraction. A) Lipid profile at 24°C. B) Lipid profile at 33°C. C) Lipid profile of different lysoPl species, upper graph at 24°C and lower graph at 33°C. Usual lipid yield for cell extracts was 6 mmoles.

Surprisingly, overexpression of *PLB3* had a major impact on the lipid profile of cells both at 24°C and 33°C, although not as initially expected. The profile of major glycerophospholipids was shifted towards phosphatidylcholine (PC) for *sec12-4* overexpressing *PLB3* at both 24°C (figure 4a) and 33°C (figure 4b), which had almost 20% more PC. This increase of PC is homogeneously distributed among all PC species, meaning no specific PC species is enriched. Regarding lysophospholipids, a modest increase in lysophosphatidylinositol (lysoPI) could be observed for *sec12-4* overexpressing *PLB3* at both 24°C (figure 4a) and 33°C (figure 4b). However, having a closer look to the major lysoPI species more acute changes can be observed (figure 4c). Both at 24°C and 33°C, an increase of more than 10% in lysoPI16:0 compared to wild type or *sec12-4* mutant. Interestingly, lysoPI16:0 is the major species of lysoPI for all measured strains.

Discussion

As shown before, overexpression of *PLB3* not only rescues growth defects in the *sec12-4* mutant (figure 1), but can also rescue the defect in ERES organization (figure 2) and ultimately helps to maintain the correct distribution of cortical ER (figure 3). This establishes a very unusual and interesting link between coat proteins and lipid metabolism, seeing that changes in lipid levels (presumably lysophospholipids) have an impact in the formation of COPII vesicles (figure 4). However, overexpression of *PLB3* cannot fully rescue the phenotypes of *sec12-4* mutant. Changes in the lipid composition are not enough to achieve vesicle formation under very compromised situations (≥35°C). These results suggest that an adequate membrane composition, perhaps enriched in conical lipids, could be one of the requirements for COPII vesicle formation. The overexpression of *PLB3* would maximize the role of lipids in vesicle formation, ultimately contributing to cell survival. Furthermore, this suggests that conical lipids could be required for optimal formation of ERES and COPII vesicle formation.

Regarding the phospholipases, only one of them had a significant impact on sec12-4 mutant survival. Interestingly, PLB3 has been proposed to exclusively catalyze the hydrolysis of PI and PS into IysoPI and IysoPS, being also less efficient than PLB1 and PLB2 (Merkel et al., 1999, 2005). Furthermore, PLB1 and PLB2 have been proposed to have Iysophospholipase activity as well, therefore hydrolyzing Iysophospholipids into glycerol phosphates and a free fatty acid(Merkel et al., 1999, 2005). It is not possible to exclude that PLB1 and PLB2 could participate as well in COPII vesicle formation under normal situations, but perhaps the overexpression of these enzymes generated toxic levels of Iysophospholipids, FFA and/or glycerol phosphates. Since PLB3 catalytic activity is not very efficient, overexpressing this enzyme could generate just enough Iysophospholipids to rescue sec12-4 mutant without

reaching toxic levels of the *PLB3* products. Further research would be required to clear up the participation of these enzymes in COPII vesicle formation under normal conditions and clarify their precise distribution in cellular compartments (Henry et al., 2012).

Interestingly, the lipidomic measurements presented in this chapter show just a modest increase in lysophospholipids and a much higher impact on PC levels (figure 4a and 4b). Although this was initially unexpected, the increase in PC may be an indirect consequence of PLB3 activity. As the lipid profile is represented as mole percent, a decrease in any lipid species would immediately increase the relative abundance of other lipids. As mentioned before, PLB3 hydrolyses exclusively PI and phosphatidylserine (PS), whose levels are noticeably reduced in the strain overexpressing PLB3 (figure 4a and b). This would increase even more the apparent abundance of PC in sec12-4 overexpressing PLB3. A possible explanation for this increase in PC could be the recycling of the excess of free fatty acids (FFA) generated by PLB3 activity. As observed in figure 4c, lysoPl16:0 levels are increased in PLB3 overexpressing strain, which most likely is a product of hydrolysis from one of the major PI species, PI 34:1 or PI 32:1, probably from both. This necessarily entails the production of FFA 16:1 and 18:1, which can later be degraded or incorporated to other lyso species, therefore generating glycerophospholipids, as PC. Therefore, I propose that the increase on PC levels are a consequence of the recycling of FFA generated by PLB3 excessive activity. A control of this would be a wild type strain overexpressing PLB3, which would clarify if the lipid profile shift is due to PLB3 overexpression only or it could be restricted to sec12-4 mutant. Perhaps PC accumulates in the ER because of a combination of both high production of PC and defects in vesicle formation (sec12-4 mutant).

Nevertheless, the preliminary mass spectrometry measurements done with the other rescue phenotypes found by Funato and collaborators suggested as well the participation of lysophospholipids as the only change in common between the two strains (not shown) (Kajiwara et al., 2013).

With regards to the ERES distribution in the cell, it was shown by Barlowe and collaborators that active lipid synthesis was required for ERES organization *in vivo* (Shindiapina and Barlowe, 2010). Also, PC and PI were required for efficient vesicle budding in *in vitro* reactions. This highlights the importance of lipids in ERES distribution and vesicle formation. The results shown in figure 2 further supports the participation of lysophospholipids in ERES organization and efficient COPII vesicle budding. However, how lysophospholipids participate in vesicle formation is not addressed by these experiments. One possibility would be by modifying bending rigidity due to an accumulation of conical lipids, which would lower the energy required to generate curved membranes, such as vesicles or ERES. Another

possibility, would be that lysophospholipids would generate packing defects that would allow Sar1p or COPII proteins to bind to the ER membrane more efficiently under limiting circumstances. Nevertheless, conical lipids and curvature can generate packing defects in membranes (Vamparys et al., 2013). Interestingly, ERES have been shown to be curved structures and to localize at the edge of deformations in the ER (Okamoto et al., 2012), which suggest the presence of packing defects and suggest that ER membrane has lower bending rigidity at these subdomains. To have a clear picture of the precise role of conical lipids in COPII vesicle formation, it would be required to first measure the lipid composition of the ER and COPII vesicles, and finally to try reconstitutions of these lipid compositions to better understand how different lipids could influence the membrane binding and deformation by COPII proteins.

Finally, it was striking to find that sec12-4 mutant had problems to organize the cortical ER under non permissive conditions. This was not shown by early reports using electron microscopy on sec12-4 mutants and others related mutants (sec23-1 or sec16-1). On the contrary, when cells were incubated at 37°C, cortical ER was found to be correctly distributed, with the only visible phenotype being extra ER cisternae accumulation on the cytoplasm (Kaiser and Schekman, 1990; Novick et al., 1980). However, in the experiments performed in this study with sec12-4 mutant at 33°C, this accumulation was not evident while the cortical ER was clearly reduced. This does not mean that ER membranes are not being accumulated in sec12-4 mutant, but perhaps another technical approach would be required to see this. Indeed, Rapoport and collaborators showed by fluorescence microscopy that mutants related to COPII vesicle formation (sec23-1, sec13-1 and sec16-1) did not have a reduction or increase in ER membranes, but a disorganization of its structure, which supports the observations found here (Prinz et al., 2000). Overall, this suggests the importance of the COPII secretion machinery for establishing a correct ER structure. Perhaps the generation of different subdomains with different lipid composition is essential for the organization of the ER as a whole. The identification of distinct lipid subdomains in the ER will require further investigation and novel technology, as the ER is one continuous lipid bilayer deformed in multiple ways and lipids can diffuse in this structure, most likely even after fixation by most chemical fixatives.

Barlowe, C.K., and Miller, E.A. (2013). Secretory protein biogenesis and traffic in the early secretory pathway. Genetics *193*, 383–410.

Barlowe, C., and Schekman, R. (1993). SEC12 encodes a guanine-nucleotide-exchange factor essential for transport vesicle budding from the ER. Nature *365*, 347–349.

Castillon, G.A., Watanabe, R., Taylor, M., Schwabe, T.M.E., and Riezman, H. (2009). Concentration of GPI-anchored proteins upon ER exit in yeast. Traffic *10*, 186–200.

Connerly, P.L., Esaki, M., Montegna, E.A., Strongin, D.E., Levi, S., Soderholm, J., and Glick, B.S. (2005). Sec16 is a determinant of transitional ER organization. Curr. Biol. *15*, 1439–1447.

Copic, A., Latham, C.F., Horlbeck, M.A., Arcangelo, J.G. D', and Miller, E.A. (2012). ER cargo properties specify a requirement for COPII coat rigidity mediated by Sec13p. Science 335, 1359–1362.

Elrod-Erickson, M.J., and Kaiser, C.A. (1996). Genes that control the fidelity of endoplasmic reticulum to Golgi transport identified as suppressors of vesicle budding mutations. Mol. Biol. Cell 7, 1043–1058.

Henry, S.A., Kohlwein, S.D., and Carman, G.M. (2012). Metabolism and regulation of glycerolipids in the yeast Saccharomyces cerevisiae. Genetics *190*, 317–349.

Kaiser, C.A., and Schekman, R. (1990). Distinct sets of SEC genes govern transport vesicle formation and fusion early in the secretory pathway. Cell *61*, 723–733.

Kajiwara, K., Ikeda, A., Aguilera-Romero, A., Castillon, G.A., Kagiwada, S., Hanada, K., Riezman, H., Muniz, M., and Funato, K. (2013). Osh proteins regulate COPII-mediated vesicular transport of ceramide from the endoplasmic reticulum in budding yeast. J. Cell Sci. 127, 376–387.

Manzano-Lopez, J., Javier, M.-L., Perez-Linero, A.M., Auxiliadora, A.-R., Martin, M.E., Tatsuki, O., Silva, D.V., Seeberger, P.H., Howard, R., Kouichi, F., et al. (2015). COPII Coat Composition Is Actively Regulated by Luminal Cargo Maturation. Curr. Biol. *25*, 152–162.

Merkel, O., Fido, M., Mayr, J.A., Prüger, H., Raab, F., Zandonella, G., Kohlwein, S.D., and Paltauf, F. (1999). Characterization and function in vivo of two novel phospholipases B/lysophospholipases from Saccharomyces cerevisiae. J. Biol. Chem. *274*, 28121–28127.

Merkel, O., Oskolkova, O.V., Raab, F., El-Toukhy, R., and Paltauf, F. (2005). Regulation of activity in vitro and in vivo of three phospholipases B from Saccharomyces cerevisiae. Biochem. J 387, 489–496.

Miller, E.A., and Schekman, R. (2013). COPII - a flexible vesicle formation system. Curr. Opin. Cell Biol. *25*, 420–427.

Montegna, E.A., Bhave, M., Liu, Y., Bhattacharyya, D., and Glick, B.S. (2012). Sec12 binds to Sec16 at transitional ER sites. PLoS One 7, e31156.

Murakami, A., Kimura, K., and Nakano, A. (1999). The inactive form of a yeast casein kinase I suppresses the secretory defect of the sec12 mutant. Implication of negative regulation by the Hrr25 kinase in the vesicle budding from the endoplasmic reticulum. J. Biol. Chem. 274, 3804–3810.

Nakano, A., Brada, D., and Schekman, R. (1988). A membrane glycoprotein, Sec12p, required for protein transport from the endoplasmic reticulum to the Golgi apparatus in yeast. J. Cell Biol. *107*, 851–863.

Novick, P., Field, C., and Schekman, R. (1980). Identification of 23 complementation groups required for post-translational events in the yeast secretory pathway. Cell *21*, 205–215.

Okamoto, M., Kurokawa, K., Matsuura-Tokita, K., Saito, C., Hirata, R., and Nakano, A. (2012). High-curvature domains of the ER are important for the organization of ER exit sites in Saccharomyces cerevisiae. J. Cell Sci. *125*, 3412–3420.

Orci, L., Ravazzola, M., Meda, P., Holcomb, C., Moore, H.P., Hicke, L., and Schekman, R. (1991). Mammalian Sec23p homologue is restricted to the endoplasmic reticulum transitional cytoplasm. Proc. Natl. Acad. Sci. U. S. A. 88, 8611–8615.

Prinz, W.A., Grzyb, L., Veenhuis, M., Kahana, J.A., Silver, P.A., and Rapoport, T.A. (2000). Mutants affecting the structure of the cortical endoplasmic reticulum in Saccharomyces cerevisiae. J. Cell Biol. *150*, 461–474.

Shindiapina, P., and Barlowe, C. (2010). Requirements for Transitional Endoplasmic Reticulum Site Structure and Function in Saccharomyces cerevisiae. Mol. Biol. Cell *21*, 1530–1545.

Vamparys, L., Gautier, R., Vanni, S., Bennett, W.F.D., Tieleman, D.P., Antonny, B., Etchebest, C., and Fuchs, P.F.J. (2013). Conical lipids in flat bilayers induce packing defects similar to that induced by positive curvature. Biophys. J. *104*, 585–593.

Chapter III:

Lipidomics analysis reveal that COPII vesicles are enriched in lysophospholipids.

The results described in the previous chapter evidence an effect of phospholipases on the stability of ERES, suggesting a participation of lysophospholipids in COPII vesicle formation. Few studies have looked into the role of lipids in COPII membrane binding and deformation. Pioneer reconstitution assays found that the lipid composition of artificial liposomes could modulate the binding of COPII coats to the membrane (Matsuoka et al., 1998). Interestingly, lysophospholipids were shown to increase Sar1 binding to liposomes. The results described on Chapter II suggest a link between lysophospholipids and COPII vesicle formation. Lysophospholipids could potentially affect membrane parameters such as bending rigidity or packing defects and increase the binding of COPII proteins to the membrane, and perhaps participate in its deformation. However, the lipid composition of COPII vesicles has been never evaluated and the possible presence of lysophospholipids is unknown. Furthermore, lysophospholipid content of the ER has not been studied as well, even though some phospholipases are in the lumen of the ER (Merkel et al., 2005). Therefore, a standing question is whether lysophospholipids are more abundant at the ER and participate in COPII vesicle formation.

I designed a strategy to obtain COPII vesicles in sufficient amount and purity to analyze their lipid composition by mass spectrometry. Taking advantage of the established techniques for cell fractionation, microsomes (fragments of the ER network) were purified from wild type yeast (figure 1). Using purified COPII minimal machinery, it is possible to generate vesicles from microsomes (Barlowe et al., 1994). One of the advantages of this cell-free assay is to reduce the possibility of cross contamination by other coated vesicles such as COPI, similar in size and carried cargo proteins, and by other organelles. The small GTPase Sar1 was purified from recombinant bacteria as previously described [see methods and (Barlowe et al., 1994)], and the heterodimers Sec23/24 and Sec13/31 were purified as sub-complexes from genetically modified yeast strains that express a C-terminal HIS-tagged Sec24 or a C-terminal HIS-tagged Sec31 (Shimoni and Schekman, 2002). Baculovirus purified yeast recombinant Sec23/24 and Sec13/31 did not generate sufficient budding yields to be used in the following.

As shown in Figure 1, these proteins were then mixed with concentrated microsomes, GTP and an ATP regenerating system. The reaction was placed at 23°C for 25 minutes, to allow for budding, and then placed on ice for 5 minutes to stop the reaction. After this incubation, an aliquot of 5% of the total reaction volume was taken for western blot analysis. Budded COPII vesicles were further isolated by centrifugation, half of the isolated vesicle suspension was used for western blot analysis and the rest was used for lipid extraction. Glycerophospholipids were extracted by standard procedures (Matyash et al., 2008) and analyzed by mass spectrometry.

Results.

Microsomes were isolated from cellular homogenates after differential centrifugation and sucrose gradient fractionation (figure 1). The concentration of microsomal proteins was assessed by absorbance at 280 nm, having an average concentration of ~3.5 mg/ml of proteins per aliquot. The microsomal fractions showed low cross contamination with mitochondrial membranes (figure 2c).

Lipidomic analysis of microsomes revealed a different glycerophospholipid composition compared to the profile of the cell (figure 2a). Microsomes are different to cells in major glycerophospholipid species, having more phosphatidylethanolamine (PE), less phosphatidylinositol (PI) and half of phosphatidylserine (PS). Lysophospholipids are more abundant on microsomes, accounting for more than 1% of their composition, lysophosphatidylethanolamine (lysoPE) being the most abundant. On the other hand, almost no lysophosphatidylserine (lysoPS) was detected.

After *in vitro* vesicle formation, all membrane fractions were collected for lipidomic analysis. Budded microsomes were separated from vesicles by high-speed centrifugation (figure 1). The lipid composition of microsomes was found to change from before to after budding reaction (figure 2b). Lysophospholipid abundance is increased in the microsomes that have been used in a budding reaction. Interestingly, no other major glycerophospholipid is changed except for PS, which severely decreases. On the other hand, only minor changes were found when microsomes were incubated with apyrase. This suggests that the increase on lysophospholipids levels on microsomes is dependent on the availability of ATP and GTP. This is consistent with an enzymatic activity hydrolyzing glycerophospholipids into lysolipids. Interestingly, ER resident phospholipases are do not dependent on nucleotides (Merkel et al., 2005). On the contrary, PS abundance is reduced in microsomes treated with apyrase, meaning that the mechanism reducing PS levels in these microsomes is independent of COPII and of nucleotides.

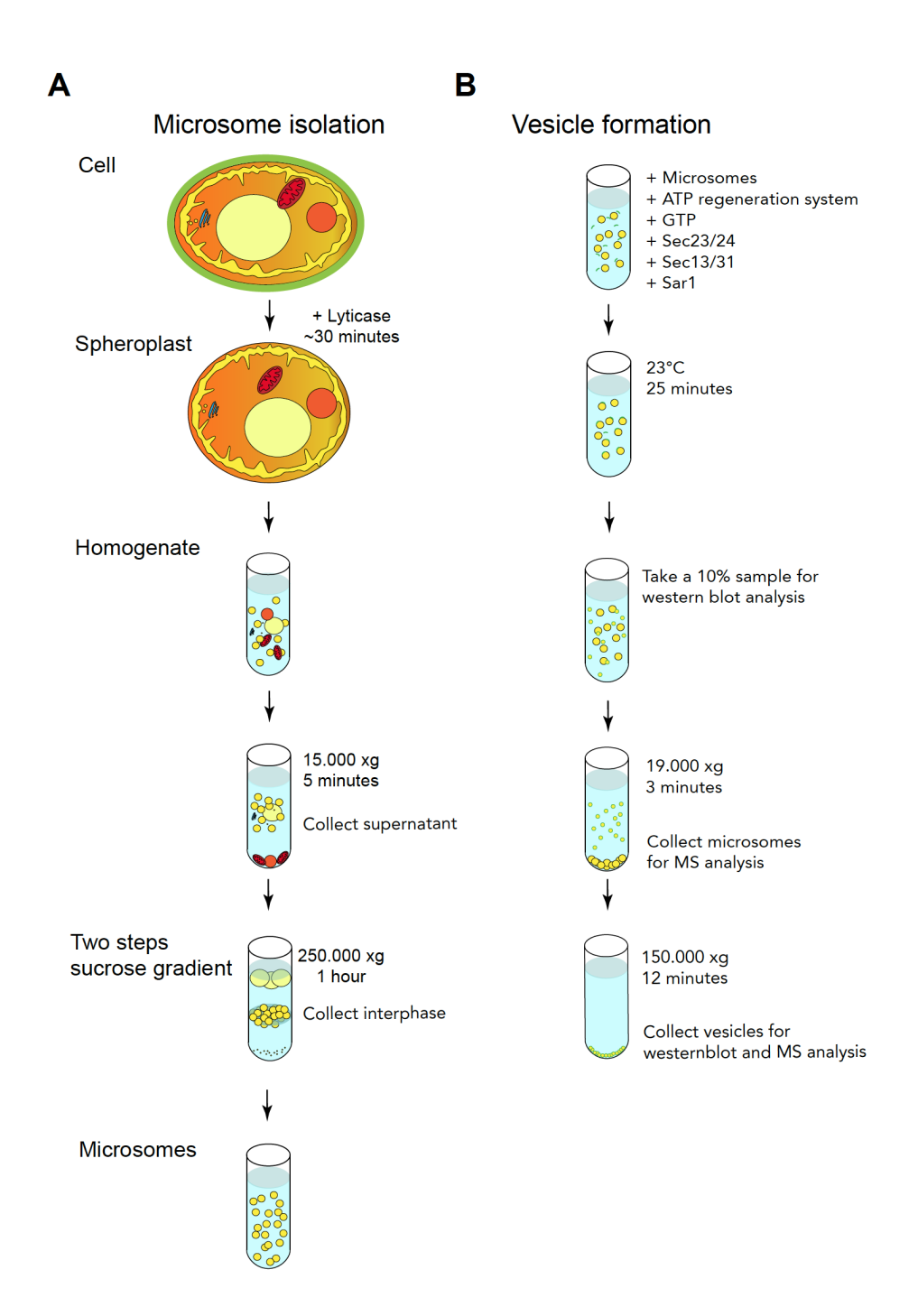


Figure 1. Procedures for microsome isolation (A) and COPII budding assay (B). All steps are carried out at 4°C except for the budding reaction itself (23°C). Microsomes are generated from a 1L yeast culture in exponential growth phase. The cell wall was digested with lyticase. Once the microsomes are isolated, 100uL concentrated aliquots (~3.5 mg/ml of protein) are kept frozen at -80°C. Two aliquots are used per COPII budding assay. In negative control reactions, COPII proteins, GTP and ATP regeneration systems are substituted by apyrase, hydrolyzing nucleotide triphosphate into monophosphate forms.

The vesicular fraction of each reaction was separated in two tubes: one was used for lipid extraction and the other half was used to analyze the efficiency of vesicle formation assay by immunoblot. For the immunoblots, vesicular cargo proteins were used as markers for COPII vesicle, such as SNAREs Sec22 and Bos1, membrane fusion protein as Erv46 or cargo recognition as Emp24. Sac1, an ER resident protein, which cannot efficiently accumulate inside vesicles, was used to test possible vesicle contamination with microsomal membranes. As shown in figure 3, few cargo or ER resident proteins were recovered when microsomes were treated with apyrase. On the other hand, cargo proteins recovery was increased by the addition of COPII machinery, GTP and ATP regeneration system (Figure 3). Therefore, despite some background of microsomal membranes, the vesicle production was very efficient.

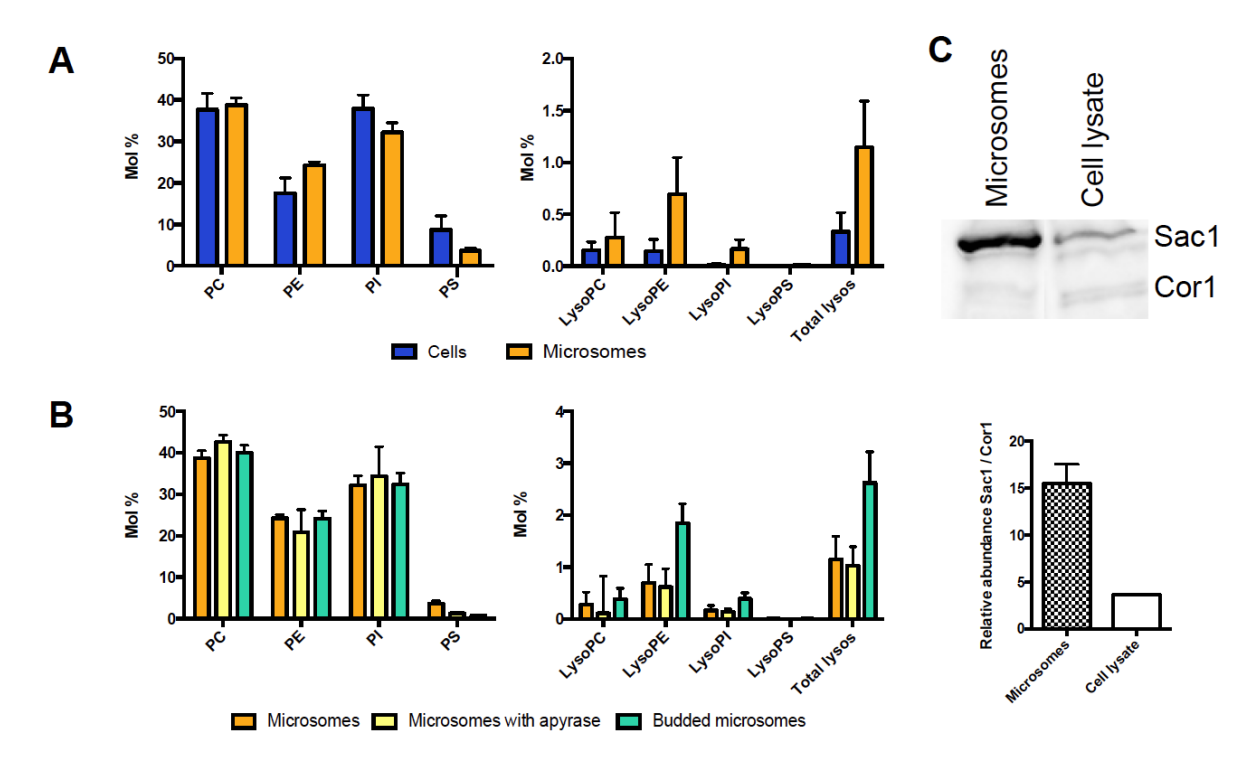


Figure 2. Profile of major glycerophospholipid classes measured by mass spectrometry (mol%). Error bars indicate standard deviation. A) Lipid profile of yeast cells (in blue, average of n=5) compared to the profile of microsomes (in orange, average of n=8). B) Lipid profile of microsomes changes after vesicle formation reaction. Orange, microsomes before reaction, yellow, microsomes incubated with apyrase (average of n=4) and green budded microsomes, those incubated with COPII proteins, GTP and ATP regeneration system, show an accumulation of lysophospholipid levels (average of n=13). C) Western blot analysis of enrichment in ER markers versus mitochondrial markers. The ratio of Sac1 (ER marker) versus Cor1 (mitochondrial marker) is represented in a graph below the blot (average of n=13, error is S.E.M.). Usual lipid yield was 2 to 5 mmoles for cells, 350 µmoles for microsomes with apyrase and budded microsomes.

The rest of the vesicle fraction was used for lipidomic analysis. Glycerophospholipids were extracted from assays done with COPII proteins or with apyrase. Before normalizing by mole percent, the lipid quantities obtained from reactions with apyrase (considered background) were subtracted from the lipid quantities of budding reactions with COPII proteins. This generated a highly reproducible lipid profile for COPII vesicles (figure 4). The profile of major glycerophospholipids was similar between vesicles and microsomes except for PS, which was lower in vesicles (figure 4a). Strikingly, COPII vesicles are enriched in lysophospholipid species, with about 4% of all glycerophospholipids. All lysophospholipid species were enriched, except for lysoPS species. LysoPE species were the most abundant microsomes lysophospholipids. When compared to budded the increase lysophospholipids was more modest but statistically significant (figure 4b).

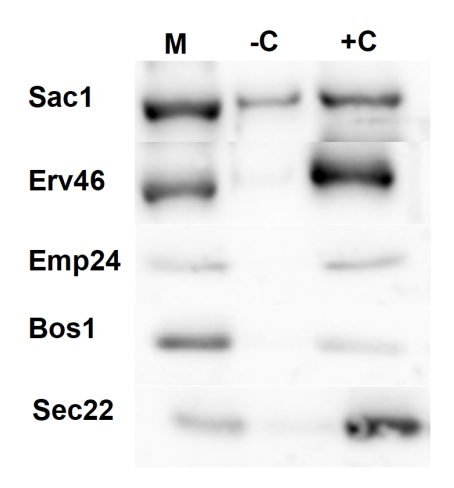


Figure 3. Cargo proteins are efficiently accumulated into *in vitro* generated COPII vesicles. In assays where no purified COPII proteins were used, the addition of apyrase blocked the formation of any background COPII vesicles (lane -C). Addition of purified COPII machinery plus GTP and ATP regeneration system generated COPII vesicles and cargo proteins can be found in the vesicular fraction (lane +C). A 5% v/v microsomal sample was loaded to estimate the initial abundance of proteins (lane M).

Next, the fold increase of each type of glycerophospholipid in vesicles was calculated (figure 4c and d). For this, two comparative ratios were done: on a first analysis, the ratio of each vesicle fraction was compared to the lipid mole percent of their batch of microsomes (figure 4c), this was done for several reactions. On a second analysis, each vesicle fraction was compared to the lipid mole percent of microsomes used in the same reaction (figure 4d), done for several reactions as well. Compared to their batch of microsomes, *in vitro* generated vesicles show a clear increase in lysophosphatidylcholine (lysoPC), lysoPE and lysoPI (figure 4c). Interestingly, lysoPI was the type of lysophospholipid that did the major change in COPII vesicles, being almost 3 times more abundant in vesicles than in microsomal membranes. On the contrary and as suggested in Figure 4a, PS and lysoPS

levels are severely reduced. When vesicles are compared to budded microsomes, the enrichment in lysophospholipids is more modest (figure 4d). Nevertheless, lysoPC and lysoPI are about twice more abundant in COPII vesicles than in the incubated microsomes. Interestingly, lysoPE shows almost no increase from incubated microsomes to vesicles. Finally, PS and lysoPS levels are lower in vesicles than in any other membrane measured, suggesting that somehow they are excluded from COPII vesicles.

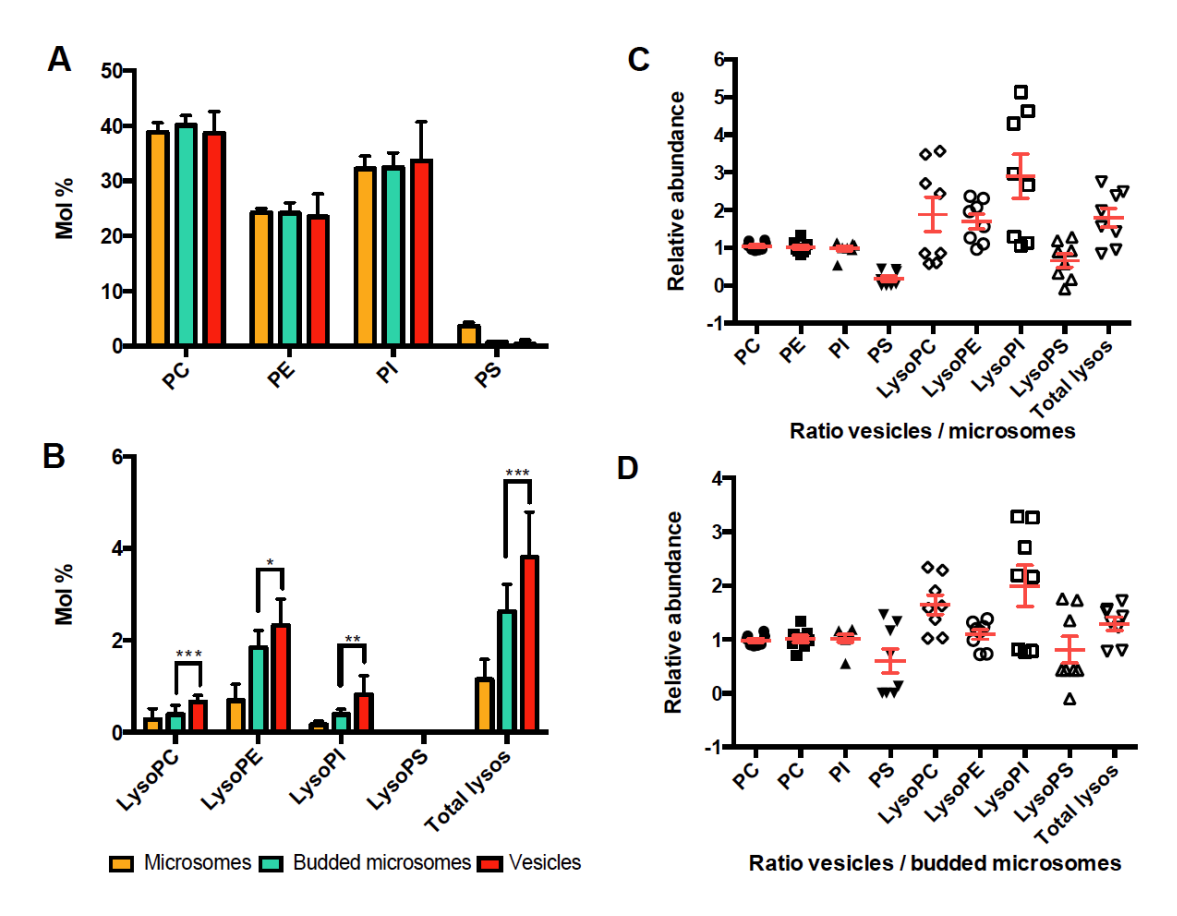


Figure 4. Mole percent of major glycerophospholipid classes measured by mass spectrometry. Error bars indicate standard deviation. A) Glycerophospholipid profile of microsomes correspond to orange bars (average of n=8), budded microsomes lipid profile is presented in green (average of n=12) and the lipid profile of *in vitro* generated COPII vesicles is shown in red. A t test was carried out to analyze the significance of these values (*= $P \le 0.05$, **= $P \le 0.01$, ***= $P \le 0.001$). C) Ratio of glycerophospholipids between different membrane fractions. The mol% for each lipid type in vesicles is divided by the mol% of the microsome batch used for that experiment, median represented in red with SEM. D) The mol% of each lipid type from vesicular fractions was divided by the mol% of the budded microsomes from the same reaction, median represented in red with SEM. Usual lipid yield was 300 µmoles for microsomes, 350 µmoles for budded microsomes and 10 µmoles.

Discussion.

COPII vesicles were successfully generated in a cell-free assay using microsomes and purified COPII proteins (figure 3). Vesicles were produced in sufficient yield for lipid extraction and analysis by mass spectrometry, and this was largely possible because of the

successful isolation of microsomal membranes. These microsomal membranes had low cross contamination from mitochondria and showed a glycerophospholipid profile similar to what had been shown before for ER organelle (Schneiter et al., 1999), with higher levels of PE and lower levels of PS than the general profile of the cell (figure 2 a and c). These results confirmed that our microsomal fraction was essentially composed of membranes originating from ER.

One of the first conclusions of this study is that lysophospholipids are more abundant at the ER than their usual abundance in yeast cellular lipid profiles. For the global glycerophospholipid content of yeast cells, lysophospholipids represent less than 0.5%. In microsomal membranes this value is clearly changed. The proportion of lysophospholipids is doubled, mostly due to the large increase in lysoPE and the appearance of lysoPI. Surprisingly, the profile of lysophospholipids changes when microsomes are incubated at 23°C and only in the presence of ATP and GTP, which suggests that glycerophospholipid remodeling requires parallel energy dependent processes (figure 2b). This may indicate that another energy dependent mechanism generates lysolipids, since yeast phospholipases are ATP and GTP independent (Merkel et al., 2005).

Interestingly, the levels of PS decrease in the process of vesicle formation, having that PS is almost absent in COPII vesicles (figures 3 and 4). Since the percentage of lysophospholipids are about the same in the profile of vesicles as the initial PS percentage of microsomes, this could be an effect of mol percent representation. However, in microsomes incubated with apyrase lysophospholipids are not changed and on the contrary PS levels are reduced. This invites to think on alternative explanations; perhaps this is due to PS specific degradation or perhaps unexplored mechanisms to sort PS out of ER exit sites (ERES) through non-vesicular PS transport (Maeda et al., 2013; Moser von Filseck et al., 2015).

The major outcome of this study is the measurement of the glycerophospholipid profile of COPII vesicles (figure 4). As proposed in the introduction, lysophospholipids are highly enriched in vesicular membranes, accounting for at least 4% of their glycerophospholipid content. Despite this percentage is not as high as other major type of lipids in the vesicle, the enrichment of lysophospholipids in COPII vesicles is many folds higher than the abundance in for cell and microsomes lipid profile. Thus, this supports the hypothesis that lysophospholipids are present in COPII vesicles at significant higher concentrations.

LysoPE is the most abundant lysophospholipid in both microsomes and vesicles, although lysoPI seems to make the major change in vesicles (figure 4). In fact, regarding the lipid ratio between vesicles and budded microsomes, lysoPI and lysoPC increase their proportion while lysoPE barely increases (figure 4d). This suggests that lysoPI and lysoPC are somehow accumulated in COPII vesicles. One thing in common between these two lysophospholipids is their extreme conical shape. Due to the steric difference in diameter

between both polar headgroups and their only acyl chain, both lysophospholipids have the most conical shape of the four types. Thus, while budding, COPII vesicle formation could concentrate extreme conical lipids, which have a shape more adapted to curved membranes. If this is true, lysoPE should be less demanded for vesicle formation due to its lower conical shape compared to the other lysos. Interestingly, this can be observed in figure 4d, where lysoPE levels barely increase from budded microsomes to COPII vesicles, just like what it is seen for PC, PE or PI, meaning that once lysoPE is generated at the microsomes it enters in vesicles as a passive passenger. Thus I hypothesized that COPII vesicles accumulate lysoPI and lysoPC due to their extreme conical shape.

LysoPI and IysoPC generated at ER membranes could accumulate at ERES and by that help in COPII membrane deformation. Interestingly, the results shown in chapter II show a modest increase of IysoPI levels in yeast overexpressing PLB3. Putting together this result with the findings shown in this chapter (Figures 4 and 5), it is reasonable to propose that IysoPI could be what alleviate sec12-4 mutant phenotype. LysoPI molecules are the most conical lipids of all Iysophospholipids and their effect on membranes could be stronger than others.

How would this facilitate COPII membrane deformation? A possible mechanism would be by lowering the bending rigidity of ER membrane, perhaps by increasing the abundance of packing defects between lipids. This has been shown for conical lipids such as di-oleyl glycerol (DOG), which has been proposed to increase the abundance and size of packing defects in flat bilayers (Vamparys et al., 2013). However the orientation of lysoPI is different to the one of DOG, being DOG inverted when compared to lipids such as lysophospholipids. The impact on lipid packing of conical lipids such as lysophospholipids has not been well studied.

Other speculative role for lysophospholipids in COPII vesicle formation could be to help to stabilize negative curvature. When membranes are deformed into a bud or a tubule, negative curvature is generated at the neck of such deformation. Lysophospholipids accumulated in the luminal leaflet of the bilayer could be sorted into this area and reduce the energy requirements for such deformation. Interestingly, the three phospholipases B characterized in yeast are proposed to be GPI anchored proteins, meaning that they are oriented towards the lumen of the ER and bound to the membrane. If the phospholipases hydrolyze lipids just in one leaflet of ER membrane, having lysophospholipids enriched in the inner leaflet of the ER is quite likely. This could potentially help to facilitate negative curvature at the neck of the vesicle.

Barlowe, C., Orci, L., Yeung, T., Hosobuchi, M., Hamamoto, S., Salama, N., Rexach, M.F.,

Ravazzola, M., Amherdt, M., and Schekman, R. (1994). COPII: a membrane coat formed by Sec proteins that drive vesicle budding from the endoplasmic reticulum. Cell 77, 895–907.

Matsuoka, K., Orci, L., Amherdt, M., Bednarek, S.Y., Hamamoto, S., Schekman, R., and Yeung, T. (1998). COPII-coated vesicle formation reconstituted with purified coat proteins and chemically defined liposomes. Cell *93*, 263–275.

Schneiter, R., Brügger, B., Sandhoff, R., Zellnig, G., Leber, A., Lampl, M., Athenstaedt, K., Hrastnik, C., Eder, S., Daum, G., et al. (1999). Electrospray ionization tandem mass spectrometry (ESI-MS/MS) analysis of the lipid molecular species composition of yeast subcellular membranes reveals acyl chain-based sorting/remodeling of distinct molecular species en route to the plasma membrane. J. Cell Biol. *146*, 741–754.

Vamparys, L., Gautier, R., Vanni, S., Bennett, W.F.D., Tieleman, D.P., Antonny, B., Etchebest, C., and Fuchs, P.F.J. (2013). Conical lipids in flat bilayers induce packing defects similar to that induced by positive curvature. Biophys. J. *104*, 585–593.

Barlowe, C., Orci, L., Yeung, T., Hosobuchi, M., Hamamoto, S., Salama, N., Rexach, M.F., Ravazzola, M., Amherdt, M., and Schekman, R. (1994). COPII: a membrane coat formed by Sec proteins that drive vesicle budding from the endoplasmic reticulum. Cell 77, 895–907.

Maeda, K., Anand, K., Chiapparino, A., Kumar, A., Poletto, M., Kaksonen, M., and Gavin, A.-C. (2013). Interactome map uncovers phosphatidylserine transport by oxysterol-binding proteins. Nature *501*, 257–261.

Matyash, V., Liebisch, G., Kurzchalia, T.V., Shevchenko, A., and Schwudke, D. (2008). Lipid extraction by methyl-tert-butyl ether for high-throughput lipidomics. J. Lipid Res. 49, 1137–1146.

Merkel, O., Oskolkova, O.V., Raab, F., El-Toukhy, R., and Paltauf, F. (2005). Regulation of activity in vitro and in vivo of three phospholipases B from Saccharomyces cerevisiae. Biochem. J 387, 489–496.

Moser von Filseck, J., Čopič, A., Delfosse, V., Vanni, S., Jackson, C.L., Bourguet, W., and Drin, G. (2015). INTRACELLULAR TRANSPORT. Phosphatidylserine transport by ORP/Osh proteins is driven by phosphatidylinositol 4-phosphate. Science *349*, 432–436.

Shimoni, Y., and Schekman, R. (2002). Vesicle budding from endoplasmic reticulum. Methods Enzymol. *351*, 258–278.

Chapter IV:

COPII proteins binding to artificial liposomes is enhanced by lysophospholipids.

As shown previously in chapters II and III, lysophospholipids are linked to COPII vesicle biogenesis. The accumulation of these conical lipids in specific areas of the membrane could modify the physical properties of the bilayer and modulate the binding of COPII coats to the surface of the endoplasmic reticulum (ER), perhaps modulating bending rigidity or increasing lipid packing defects. Unfortunately, observation of COPII binding dynamics is not accessible in complex experimental systems as living cells or semi in vitro reactions. On the other hand, in vitro approaches using artificial liposomes have proven to be extremely useful to reconstitute protein binding to liposomes. Reconstitutions using chemically defined liposomes have explored COPII membrane binding dynamics and scaffolding (Antonny et al., 2001; Matsuoka et al., 1998). Binding of Sec23/24 and Sec13/31 was found to be enhanced by the presence of anionic glycerophospholipids like phosphatidylserine (PS) and phosphatidylinositol phosphates (PIPs). Interestingly, the same study showed that Sar1 binding was modulated by membrane fluidity as liposomes containing conical lipids such as dioleoyl phosphatidic acid (DOPA) and lysophospholipids increased the binding of Sar1 to membrane. On the other hand, binding was decreased when more saturated lipid species were used. This evidence suggests a link between COPII machinery and membrane fluidity. More recently, COPII membrane remodeling has been observed with fluorescent microscopy thanks to the use of giant unilamellar vesicles (GUVs) and cryoelectron microscopy (Bacia et al., 2011; Daum et al., 2014). Using non-hydrolyzable GTP analogs, long and rigid tubules were generated from GUVs by COPII polymerization. The number and stiffness of these deformations was found to be dependent on lipid composition, with the presence of anionic phospholipids being required. Thus, there is a direct link between coat organization and lipid composition. Therefore, I addressed the question of whether lysophospholipids can modulate the binding of purified COPII components on GUVs using COPII reconstitution assays, where Sar1 and Sec13/31 were observed by fluorescent microscopy.

Results.

First, the binding and polymerization on GUVs of purified COPII proteins was observed by confocal microscopy. GUVs with lipid composition similar to the major-minor mix (DOPC 34.4%, DOPE 14.8%, PI 5.4%, DOPS 5.4%, DOPA 3.4%, PI(4)P 1.5%, PI(4,5)P₂ 0.5%,

CDP-DAG 1.3% and cholesterol 33%, including 0.1% of Rhodamine-PE) were generated by electroformation. COPII proteins were purified from yeast strains as described in materials and methods. To visualize COPII machinery, Sar1 was chemically labelled with maleimide Atto 647 (Atto-tec product no. AD 647N-3) and Sec13/31 was labelled with TFP-Alexa-488 (Life technologie product no. A37563), while Sec23/24 remained unlabelled. Sar1 was combined with Sec23/24 and Sec13/31 in buffer B88 (HEPES 20mM, sorbitol 250mM, Potassium Acetate 150mM, Magnesium Acetate 5mM, pH 6.8). The non-hydrolyzable GTP analog GTP γ S and magnesium were used promote Sar1 binding to GUVs after inducing the release of GDP for GTP γ S with 2.5mM EDTA. The mix of proteins including activated Sar1 was loaded in a microfluidic chamber (ibidi μ -Slide) precoated with BSA. Finally, GUVs were added to the mix and observed with a spinning disc confocal microscope.

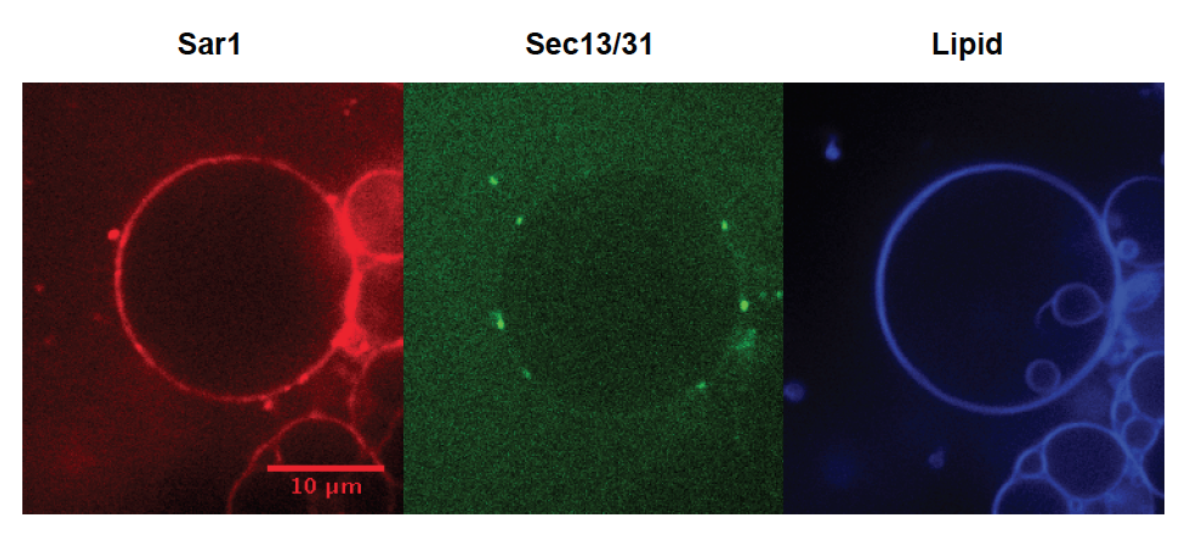


Figure 1. COPII polymerization on GUVs. Each assay was composed of Sar1-Atto647 (0.75 μ g/ μ I), Sec23/24 (0.25 μ g/ μ I), Sec13/31 (0.18 μ g/ μ I) and Sec13/31-Alexa488 (0.18 μ g/ μ I). COPII proteins were mixed and Sar1 was activated with 2.5mM EDTA in low Mg²⁺ B88 and GTP γ S 1mM. After 30 minutes of incubation with GUVs, fast acquisitions were obtained using spinning disc confocal microscope. Sar1 (in red) homogeneously binds to the complete surface of a GUV while Sec13/31 forms discrete loci. Lipid bilayer shape (in blue) was not modified by COPII coats.

After few minutes of incubation, Sar1 was found to cover the surface of GUVs homogeneously (figure 1). On the contrary, longer time (>30min) was needed for Sec13/31 to bind (figure 1). Many GUVs presented dot structures of Sec13/31 bound to the surface although some GUVs did not present any Sec13/31 bound (figure 2a). The loci formed by Sec13/31 were mobile and corresponded to a light accumulation of Sar1 at the same spot. No accumulation of membrane was seen at the spot of Sec13/31, suggesting that if any membrane deformation occurred, it would be fairly limited. Longer incubations (>2h) did not change the number or size of Sec13/31 structures, nor generated any membrane deformation such as tubules.

In order to test whether IysoPI affects COPII coat organization, major-minor mix was modified to include 10% of soy IysoPI (with IysoPI16:0 as the major species), which acylchain distribution was close to the one of yeast. To make this composition, 10% of DOPC was substituted by 10% of IysoPI. Proteins and GUVs were mixed and observed in the same conditions as experiment in figure 1. Surprisingly, the distribution of both Sar1 and Sec13/31 was different when using GUVs with 10% IysoPI. After 30 minutes of incubation, Sar1 covered the surface of GUVs (figure 2b). However the distribution was not completely homogeneous and small and highly mobile dots were observable (figure 2b and figure 3). Strikingly, Sec13/31 was found to be distributed in a similar way to Sar1 (figure 2b). Moreover, the peaks of fluorescence signal around the contour of the GUVs clearly showed that Sec13/31 was bound to the surface (figure 2 c and d). High accumulations of Sar1 and Sec13/31 were found at lipid aggregates (figure 2b) or at intersections between two GUVs (figure 1), both with and without Iysophospholipids and were probably unspecific protein aggregates. Finally, no remarkable deformations or differences in the shape of GUVs was found under these conditions.

The scattered distribution of both Sar1 and Sec13/31 on GUVs with IysoPI was further characterized. Doing fast acquisitions of the three fluorophores it was observed that some of the spots of Sar1 were close to dots of Sec13/31 (figure 3), meaning that probably both dots are at the same position. Faster acquisitions are required to further characterize this. Time frame images showed these dots were moving around the surface of the GUV (figure 3b).

Finally, not all GUVs with 10% lysoPI had the same binding of Sec13/31. Interestingly, those GUVs with lysoPI that had a distribution of Sar1 similar to the observed for GUVs without lysoPI, the binding of Sec13/31 was visibly weaker (figure 3a, lower left GUV). Perhaps this is due to composition inhomogeneities in the population of GUVs.

Taking together these results, one conclusion is that lysophospholipids do increase the binding of Sec13/31 to membrane surface. Moreover, Sar1 and Sec13/31 have a scattered distribution in the presence of lysophospholipids.

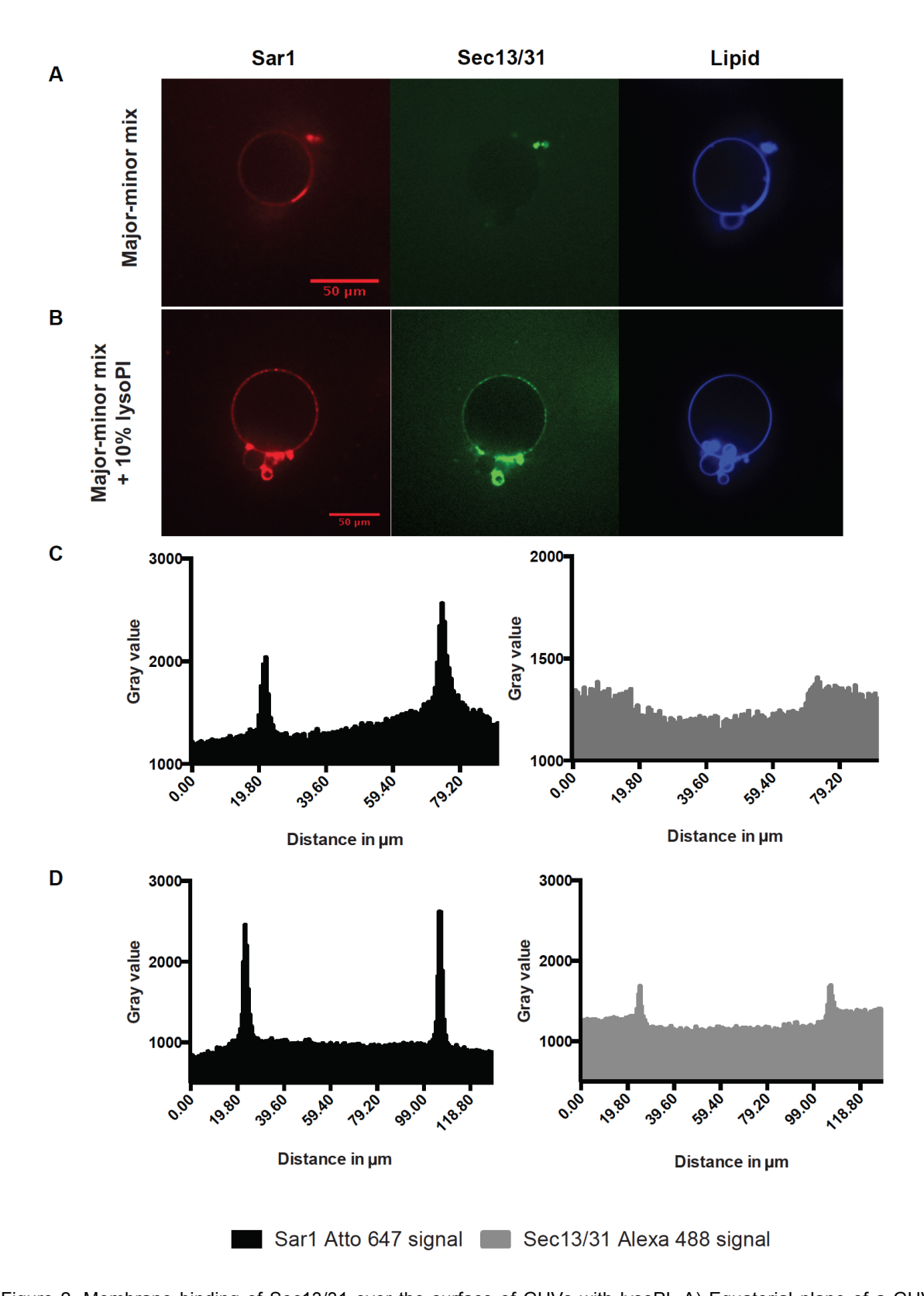


Figure 2. Membrane binding of Sec13/31 over the surface of GUVs with IysoPI. A) Equatorial plane of a GUV without IysoPI shows binding of Sar1 but no Sec13/31. B) Equatorial plane of GUV with 10% IysoPI shows binding of Sar1 and Sec13/31 in similar experimental conditions as in A. C) Profile of Sar1 and Sec13/31 fluorescent signals of the GUV shown in A. D) Profile of Sar1 and Sec13/31 fluorescent signal of the GUV shown in B. Peaks for Sec13/31 can be appreciated on the contour of the GUV.

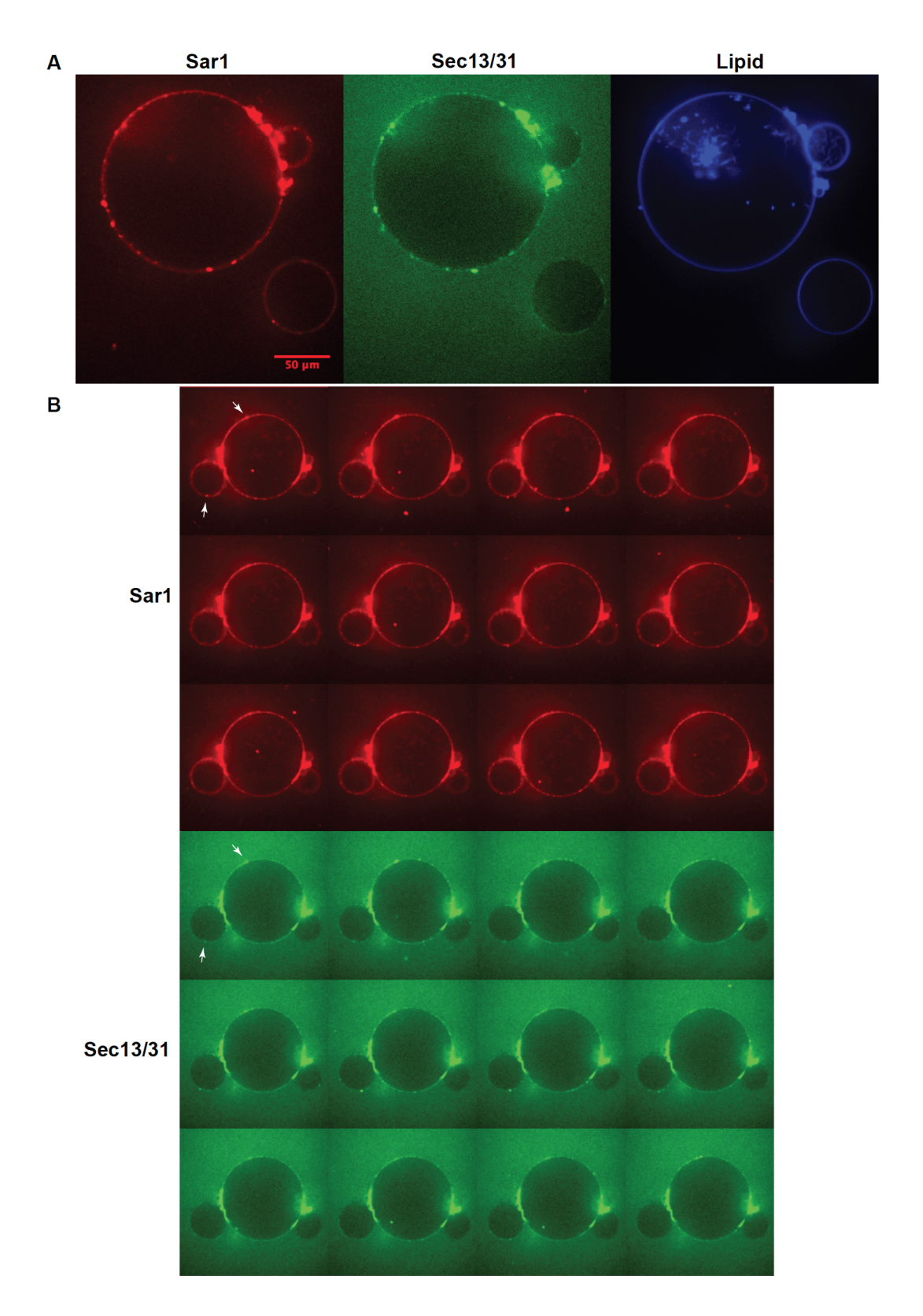


Figure 3. Binding of COPII proteins is not completely homogeneous in GUVs composed of major-minor mix +10% lysoPI. A) Sar1 and Sec13/31 are not distributed homogeneously. Accumulations of both proteins can be found and have a similar distribution at the same time. B) The dots of Sar1 and Sec13/31 (arrows) are mobile and change position through the surface of the GUVs. Time-lapse images (5 seconds per frame) show the movement of dots over the surface. Time course from left to right and up to down.

Discussion.

In light of the experiments shown above, it is possible to conclude that COPII polymerization is enhanced by the presence of lysophospholipids on the membrane. Previous studies showed that binding of Sec23/24 and Sec13/31 is dependent on anionic glycerophospholipids (Matsuoka et al., 1998), and under these conditions COPII is able to deform the bilayer into rigid tubules (Bacia et al., 2011; Daum et al., 2014). However, this is not was has been found in the experiments of this chapter. In GUVs with standard majorminor composition (identical to previously published except for the use of cholesterol instead of ergosterol), Sec13/31 was found to accumulate in isolated dots over the surface of GUVs (figure 1) and in some occasions was not present at all (figure 2a). The difference of these results compared to the previously published ones may be related to differences in protein ratios and perhaps the formation of GUVs. Nevertheless, the conditions shown in this chapter were reproducible and established an assay where the impact of lysophospholipids could be explored.

Sar1 was found to bind homogeneously over the surface of the GUVs composed of major-minor mix (figure 1 and 2a). Strikingly, when IysoPI is in GUVs the distribution of Sar1 is slightly scattered in dots (figure 2b). Moreover, Sec13/31 binds to these giant liposomes and has a similar distribution to Sar1. Although the binding of Sec13/31 seems to be less than Sar1 (figure 2d), both the GTPase and the heterodimer seem to interact together on the surface of GUVs (figure 3). Furthermore, these dots were more mobile than those found in GUVs without IysoPI, but on the contrary they were smaller in size and highly mobile (figure 3 a and b). This strongly suggests that the scaffolding of COPII coats is modified by the presence of Iysophospholipids. Interestingly, not all GUVs with IysoPI had strong binding of Sec13/31, nor the same number and size of dots. This could be due to composition heterogeneities within the population of GUVs or in individual differences on lipid composition. A precise quantification is needed to better understand the size and distribution of these dots.

How could lysophospholipids modulate COPII binding? Perhaps this is due to a change in membrane rigidity produced by the presence of lysophospholipids. These conical lipids would increase the fluidity of membranes and perhaps induce packing defects on its surface, which would lower the rigidity of the membrane and therefore lower the energy required for COPII proteins to scaffold and deform the bilayer. Further measurements of bending rigidity with optical tweezers and *in silico* simulations are required to analyze the possible

differences between lipid bilayers with and without lysoPI. Previous studies showed that binding of COPI coat to giant liposomes is favoured by low tension and low rigidity (Manneville et al., 2008), most likely COPII coats would have similar requirements and it will be interesting to explore how changes in membrane tension and different lipid compositions affect COPII polymerization.

Another open question is whether Sec23/24 is also found in these dots. Most likely the distribution will be similar between all COPII proteins since they act as a complex. Nevertheless, it would be worthwhile to have a more complete data.

Since no obvious membrane deformation has been observed, this suggests that something is missing in these reconstitutions or perhaps the lipid composition is not completely optimal. Regarding the major-minor mix, it would be interesting to modify the ratio several lipids and try to adjust it to the lipid profile established for COPII vesicles in chapter III, increasing the ratio of phosphatidylinositol and lowering the levels of phosphatidylserine, PIPs and sterols. Increasing and lowering the ratio of lysoPI would help as well in understanding the role of these conical lipids in COPII polymerization.

Several experimental controls are required to further study Sar1 binding. It would be interesting to know how GTP or GDP Sar1 forms behave in the presence of lysophospholipids. It was shown before that unspecific binding of Sar1-GDP was increase by the presence of lysophospholipids. It would be interesting to observe and quantify this by confocal microscopy.

Antonny, B., Madden, D., Hamamoto, S., Orci, L., and Schekman, R. (2001). Dynamics of the COPII coat with GTP and stable analogues. Nat. Cell Biol. *3*, 531–537.

Bacia, K., Kirsten, B., Eugene, F., Simone, P., Annette, M., Sebastian, D., Daniela, G., Briggs, J.A.G., and Randy, S. (2011). Multibudded tubules formed by COPII on artificial liposomes. Sci. Rep. 1.

Daum, S., Sebastian, D., Daniela, K., Annette, M., Jan, A., Simone, P., Briggs, J.A.G., and Kirsten, B. (2014). Insights from reconstitution reactions of COPII vesicle formation using pure components and low mechanical perturbation. Biol. Chem. 395.

Manneville, J.-B., Casella, J.-F., Ambroggio, E., Gounon, P., Bertherat, J., Bassereau, P., Cartaud, J., Antonny, B., and Goud, B. (2008). COPI coat assembly occurs on liquid-disordered domains and the associated membrane deformations are limited by membrane tension. Proc. Natl. Acad. Sci. U. S. A. *105*, 16946–16951.

Matsuoka, K., Ken, M., Lelio, O., Mylène, A., Bednarek, S.Y., Susan, H., Randy, S., and Thomas, Y. (1998). COPII-Coated Vesicle Formation Reconstituted with Purified Coat Proteins and Chemically Defined Liposomes. Cell *93*, 263–275.

Chapter V: Discussion and conclusions.

Our hypothesis is that lysophospholipids are not completely passive passengers of early secretory vesicles. On the contrary, these conical lipids could participate in COPII vesicle formation and facilitate efficient coat protein binding and membrane deformation. The experimental evidence described in previous chapters point to lysophosphatidylinositol (lysoPI) as a possible partner of COPII coats. In this study, high amount of lysophospholipids have been found in COPII vesicles and lysoPI levels have been functionally linked to vesicle formation and COPII proteins binding to membrane.

As described in chapter II, defects in endoplasmic reticulum exit sites (ERES) and COPII vesicle formation are rescued by overexpression of a phospholipase, PLB3, which specifically hydrolyzes phosphatidylinositol (PI), releasing in turn lysoPI and a free fatty acid. Strikingly, these cells accumulated more phosphatidylcholine (PC) and lysoPl, plus they improved fitness of the sec12-4 mutant when growing above non permissive temperatures. Lipidomic analysis of ER membranes and COPII vesicles showed that vesicles are four fold enriched in lysophospholipids when compared to the donor membranes of the ER. Interestingly, the largest fold changes in lipid profile from ER to COPII vesicle were found in lysoPI and lysoPC. The structural connection between these two lipid types suggest that it is their conical shape that might facilitate their accumulation inside COPII vesicles, since other less conical varieties like lysophosphatidylethanolamine (lysoPE) did not change levels from the ER to COPII vesicles. In the previous chapter, the influence of lysoPI in COPII binding to artificial liposomes was studied. To this end, lysoPI from soybeans was used, which is mostly composed by lysoPI16:0. With the experimental conditions that were used, those artificial liposomes with 10% of lysoPI in its composition had not only increased binding of coat proteins to the surface, but also they were arranged in different structures when compared to those artificial liposomes without lysophospholipids. Small and highly mobile structures of Sar1 and Sec13/31 appeared on the surface. Compiling these results, lysoPI appears to be involved in COPII vesicle formation and could potentially modulate coat binding to the ER surface or ER exit sites. Interestingly, lysoPI16:0 is the most abundant lysoPI available in yeast cells and is as well the most conical lysophospholipid.

It is quite likely that the accumulation of extreme conical lipids such as IysoPI16:0 will have an impact on the physical properties of membranes. The data presented in chapters II and IV suggest that Sar1 binding dynamics could be modulated by the presence of Iysophospholipids. Similar observations were previously reported (Matsuoka et al., 1998). In fact, it was found that membrane fluidity had an impact in Sar1 membrane binding. Thus, it is probable that the *sec12-4* rescue via *PLB3* overexpression and the results in reconstituted

systems are both a consequence of a direct increase in local membrane fluidity due to an increase in lysophospholipids, especially lysoPI. Moreover lysophospholipids are probably lowering the bending rigidity of membranes, thus helping the other coats Sec23/24 and Sec13/31 to deform ER membrane. Interestingly, Sar1 has been found to lower membrane rigidity (Settles et al., 2010), which supports the idea that a lower bending rigidity is probably required for COPII to deform ER membrane.

At last, lysos could participate in the fission step of vesicle formation. Prior to pinch off from the ER, an extremely curved bilayer with a narrow diameter connects the vesicle to the ER membrane. Perhaps lysophospholipids may sort to this neck and help to destabilize the membrane and promote fission. This speculative model could be studied *in silico* and will give important information about the enigmatic fission step in COPII vesicle formation.

Further research will be required to fully understand the mechanism by which COPII protein function is linked to IysoPI. One speculative hypothesis is that phospholipases may be more active at ERES. Many reports have shown that phospholipase activity is enhanced by packing defects (Grandbois et al., 1998) which can be generated by curvature. Perhaps curved ERES and COPII buds enhance the activity of these phospholipases and this way favour membrane deformation by modulating lipid composition. Another possible explanation could be that Iysophospholipids are generated elsewhere and are accumulated at the ERES and vesicles due to their shape. Lysophospholipid sorting is not well documented and further research is required to get an idea if this hypothesis is reasonable.

The lipidomics performed on ER membranes has validated most of the results obtained in previous studies (Schneiter et al., 1999) and has provided new information regarding the lysophospholipid content. An experimental design combining classical biochemical approaches with current lipidomic techniques has made possible to obtain the first lipidome of COPII vesicles. Another limitation of this experimental setup is the possibility that COPII vesicle may not be generated from native ERES. ERES might be disrupted in the process of microsome generation. Even if ERES integrity resist the fractionation process, saturating budding conditions may lead to non specific formation of COPII vesicles elsewhere outside the preformed ERES (potentially including a different lipid composition, cargo proteins and coat regulators such as Sec16). Therefore, the profile obtained in this study is a first attempt of COPII lipidome done with state of the art approaches. Most likely, those lipids that are enriched over the lipids of the donor membrane are more likely to be specific to COPII membrane. Thus, one speculation could be that levels of lysophospholipids in in vivo formed COPII vesicle may be higher than those for in vitro vesicles obtained here. In vitro reconstitutions may be helpful to establish a threshold of lysophospholipids required for COPII binding and/or membrane deformation.

Experimentation with artificial liposomes will give more information on the physical properties of lysophospholipids and their effect on lipid bilayers. Additionally, reconstitution of COPII system is still in its initial stages and could render exceptional support to understand the function of this coat complex. It would be of tremendous interest to study the binding preference of COPII coats regarding tension and membrane phase behaviour, as has been done for COPI (Manneville et al., 2008).

Possibly, more lipids could have a close functional relationship with COPII vesicles. In this thesis we have explored the effects related to lysophospholipids, but previous works have found that active glycerophospholipid synthesis is required for ERES stability (Shindiapina and Barlowe, 2010). It is quite likely that acyl chain unsaturations may be important as well for ERES conformation and vesicle biogenesis. Furthermore, not all the lipids synthesized in the ER are exported through COPII vesicles and only now researchers are grasping the mechanism for such non-vesicular pathways. Understanding such lipid sorting and the mechanisms related to it will probably bring more knowledge about what defines a COPII vesicle.

Grandbois, M., Michel, G., Hauke, C.-S., and Hermann, G. (1998). Atomic Force Microscope Imaging of Phospholipid Bilayer Degradation by Phospholipase A2. Biophys. J. 74, 2398–2404.

Manneville, J.-B., Casella, J.-F., Ambroggio, E., Gounon, P., Bertherat, J., Bassereau, P., Cartaud, J., Antonny, B., and Goud, B. (2008). COPI coat assembly occurs on liquid-disordered domains and the associated membrane deformations are limited by membrane tension. Proc. Natl. Acad. Sci. U. S. A. *105*, 16946–16951.

Matsuoka, K., Orci, L., Amherdt, M., Bednarek, S.Y., Hamamoto, S., Schekman, R., and Yeung, T. (1998). COPII-coated vesicle formation reconstituted with purified coat proteins and chemically defined liposomes. Cell *93*, 263–275.

Schneiter, R., Brügger, B., Sandhoff, R., Zellnig, G., Leber, A., Lampl, M., Athenstaedt, K., Hrastnik, C., Eder, S., Daum, G., et al. (1999). Electrospray ionization tandem mass spectrometry (ESI-MS/MS) analysis of the lipid molecular species composition of yeast subcellular membranes reveals acyl chain-based sorting/remodeling of distinct molecular species en route to the plasma membrane. J. Cell Biol. *146*, 741–754.

Settles, E.I., Loftus, A.F., McKeown, A.N., and Parthasarathy, R. (2010). The vesicle trafficking protein Sar1 lowers lipid membrane rigidity. Biophys. J. 99, 1539–1545.

Shindiapina, P., and Barlowe, C. (2010). Requirements for Transitional Endoplasmic Reticulum Site Structure and Function in Saccharomyces cerevisiae. Mol. Biol. Cell *21*, 1530–1545.

Chapter VI: Materials and methods.

Strains and materials.

Yeast strains:

YPH499 (MATa ade2 trp1 ura3 leu2 his3 lys2).

SMY80 (*MATa sec12-4 ade2 trp1 ura3 leu2 his3 lys2*) kindly provided by Akihiko Nakano (Okamoto et al., 2012).

KMY111 (SMY80 SEC13-GFP::TRP1) kindly provided by Akihiko Nakano (Okamoto et al., 2012).

BY4742 ($MAT\alpha\ his3-\Delta 1\ leu2-\Delta 0\ lys2-\Delta 0\ ura3-\Delta 0$).

BY4741 (MATa his3- Δ 1 leu2- Δ 0 met15- Δ 0 ura3 Δ -0).

RSY1069, used for Sec23/24 purification. Kindly provided by Charles Barlowe.

CBY120, used for Sec13/31 purification. Kindly provided by Charles Barlowe.

Bacteria strains:

DH5 α , used for plasmid replication.

RSB805, used for lyticase purification. Kindly provided by Charles Barlowe.

CBB205, with GST-Sar1 fusion expression plasmid pTY40. Kindly provided by Charles Barlowe.

Plasmids:

pRS425-GDP

pRS425-GDP-PLB1 (into BamHI-Sall)

pRS425-GDP-PLB2 (into Spel-Xhol)

pRS425-GDP-PLB3 (into Pstl-Sall)

YCPLAC-SEC13mch

Antibodies:

αBos1 (Riezman lab).

αEmp24 (Riezman lab).

αErv46 (Barlowe lab).

αSac1 (Barlowe lab).

αSec22 (Barlowe lab).

Experimental procedures.

ERES visualization:

YPH499 was transformed with YPCLAC-*SEC13mch* to visualize ERES in wild type yeast. KMY111 was transformed with pRS425-*PLB3* and used to visualize ERES in *sec12-4* mutant. KMY111 alone was used as a negative control. Strains were grown at 24°C in minimal media until 0.5 OD₆₀₀/ml and then collected and resuspended in YPD media. Each culture was divided in two and one half was placed at 30°C. At that moment, a sample of each strain incubated at 24°C was observed using a Zeiss Axio Z1 epifluorescence microscope. Random cells were chosen and well defined endoplasmic reticulum (ER) exit sites (ERES) were counted manually. After 30 minutes incubation at 30°C, a sample of each strain was taken and placed on glass slides prewarmed at 30°C. The 3 strains were observed and analyzed in the same way as described before.

Electron microscopy:

Strains YPH499, SMY80 and SMY80 transformed with PLB3 plasmid were incubated overnight in minimal media at 24°C. The three cultures were subcultured into YPD media and at 0.5 OD₆₀₀/ml the cultures were transferred to 33°C for 30min. After this time, cells were fixed (2,5% glutaraldehyde/tp PO4 0,1M for 1 hour) and were further treated with 2% osmium tetroxide in buffer and immersed in a solution of uranyl acetate to enhance contrast of membranes. The pellets were dehydrated in increasing concentrations of ethanol followed by pure propylene oxide, then embedded in Epon resin. Thin sections for electron microscopy were stained with uranyl acetate and lead citrate.

Protein purifications.

Lyticase was produced from bacteria using strain RSB805, gently provided by Charles Barlowe. An overnight preculture in LB media with ampicillin was diluted 1/100 in 6x 1.5 L of Super Broth medium with ampicillin. At OD₆₀₀ 0.4 to 0.6, lyticase overexpression was induced with IPTG at 1mM final concentration. Cells were harvested 4 hours later (5 min 5k rpm, GS-3 rotor) and stored at -80°C. Pellet was resuspended in 500 ml 25mM Tris/HCl pH 7.5 and then centrifuged (10 min 5k rpm in GS-3 rotor) at 4°C. Pellet was resuspended in 180ml 25mM Tris/HCl pH 7.5, 2 mM EDTA. Then, 180 ml of 40% sucrose solution were added. The mix was shaken for 20 min at room temperature. Pellet down at 7500 rpm for 10 minutes at 4°C. Supernatant was discarded and pellet was resuspended in 180 ml of cold 0.5 mM MgSO₄, then shaked at 4°C for 20 min. Centrifuge in Beckman GSA 25.50 tubes for 10 minutes at 10.000 rpm. Collect supernatant and dialyze for 3 hours at 4°C against 1 L

50mM NaOAc pH 5, then overnight in same volume fresh buffer. Lyticase preps were aliquoted in 15ml Falcon tubes and frozen in liquid nitrogen. Finally stored at -80°C.

Sar1 was purified from CBB205 transformed with PTY40, a GST-Sar1p fusion expression plasmid. The strain was plated on LB plus ampicillin and grow 37°C overnight. 200ml of LB media plus ampicillin were inoculated. At 0.7 OD₆₀₀/ml, expression was induced by addition of IPTG 0.5mM final. The culture was incubated 3 hours at 37°C. After this, cells were collected by centrifugation and the pellet was frozen at -80°C. The pellet was resuspended in Tris-buffered saline (TBS) solution (Tris 50nM, NaCl 150mM, MgCl₂ 5mM plus 1% Triton x100, at pH 7.4). Afterwards, the sample was sonicated 3 cycles for 3 minutes. Then, the sample was centrifuged at 12.000 xg for 30min and collect supernatant. A bed of 7ml of glutathione sepharose beads was added and incubated in rotatory agitation for 1 hour at 4°C. TBS (no detergent) and glutathione 30mM were added at pH 7.4. Fractions of 1ml were manually collected and analyzed by SDS-PAGE and coomassie stained. Peak fractions were pooled and 150µl of PreScission at 1.5mg/ml were added. Supernatant was dialyzed 2 hours against B88 buffer (HEPES 20mM, sorbitol 250mM, Potassium Acetate 150mM, Magnesium Acetate 5mM, pH 6.8) plus GDP 5µM. A bed of 7ml of glutathione sepharose beads was added. The mix was incubated 1 hour at 4°C in rotatory agitation. After this, the supernatant was injected in a BioRad GST-kit column, collecting the flow through. Protein concentration was estimated by BCA and aliquots of 10µl were frozen in liquid N2 and stored at -80°C.

Sec23/24 was purified using yeast strain RSY1069, gently provided by Charles Barlowe. A yeast preculture was grown overnight in SD+Ade+His at 30°C. Yeast were subcultured at $0.005~OD_{600}/ml$ in 21L SD+Ade+His and incubated using a fermentor at 30°C with air supply. Cells were collected at 1.65 OD₆₀₀/ml and collected by centrifugation at 5k rpm, 5 min at 4°C.Pellets were frozen at -80°C. Approximately 40gr of yeast were obtained. Cells were pulverized using a Retsch MixerMill 400, liquid nitrogen cold. The power was resuspended in 100 ml lysis buffer (Hepes KOH 50mM, Potassium Acetate 750mM, EGTA 0.1mM, glycerol 10%, PMSF 0.5mM, β-mercaptoethanol 1.4mM, pH 7) with protease inhibitor cocktail. Then it was centrifuged 40.000 xg for 1 hour. After centrifugation, lipid top layer was removed by aspiration. The lysate was injected on a HiTrap Imac 1ml column. Then washed with MES 50mM, Potassium Acetate 750mM, EGTA 0.1mM, imidazole 40mM, glycerol 10% and β-mercaptoethanol 1.4mM (pH 7). Next washed with HEPES 50mM, Potassium Acetate 500mM, EGTA 0.1mM, imidazole 40mM, glycerol 10% and β-mercaptoethanol 1.4mM (pH 7). Then washed with HEPES 50mM, Potassium Acetate 500mM, EGTA 0.1mM, imidazole 100mM, glycerol 10% and β-mercaptoethanol 1.4mM (pH 7).

7). Proteins were eluted with HEPES 50mM, Potassium Acetate 500mM, EGTA 0.1mM, imidazole 400mM, glycerol 10% and β -mercaptoethanol 1.4mM (pH 7). Fractions of 1ml were collected. A SDS-PAGE plus coomassie stain was done to determine the fractions containing proteins. The fractions were combined and dialyzed overnight in HEPES 50mM, Potassium Acetate 500mM, EGTA 0.1mM, imidazole 100mM, glycerol 10% and β -mercaptoethanol 1.4mM (pH 7). The product of dialysis was injected in an ion-exchange (HiTrap DEAE) 1ml column. The injection buffer was HEPES 50mM, Potassium Acetate 500mM, EGTA 0.1mM, imidazole 50mM and glycerol 10% (pH 7). The elution buffer had HEPES 50mM, Potassium Acetate 1M, EGTA 0.1mM, imidazole 50mM and glycerol 10% (pH 7). The elution was done with 80% elution buffer 20% injection buffer. Fractions of 1ml were collected. A SDS-PAGE plus coomassie stain was done to determine the fractions containing Sec23/24. Fractions A2 to A6 were pooled and dialyzed against HEPES 50mM, Potassium Acetate 800mM and Magnesium Acetate 5mM (pH 7.4).

Sec13/31 was purified from CBY120, gently provided by Charles Barlowe. The strain was incubated at in 10ml SD-Ura at 30°C. About 24 hours after, cells were subcultured in 2L SD-Ura and incubated at 30°C. At the next day, the culture was diluted in 19L of YPD in a fermentor with air supply at a final OD₆₀₀/ml of 0.12. The cells were collected at the next morning at 2.3 OD₆₀₀/ml, after centrifugation the pellet was frozen at -80°C. About 90gr of cells were collected. Cells were pulverized using a Retsch MixerMill 400, liquid nitrogen cold. The pellet was resuspended in cold B88 buffer (HEPES, 50mM, Potassium Acetate 150mM, sorbitol 250mM, Magnesium Acetate 5mM at pH 7) and centrifuged at 10.000 xg for 10min. After this, the supernatant was further centrifuged at 100.000 xg for 1 hour. After centrifugation, a top layer of lipids was removed by aspiration and the rest of the supernatant was injected in a histidine trap Imac column of 5ml. Two buffers were used, Buffer A (HEPES 20mM, Potassium Acetate 150mM, pH 7), and Buffer B (HEPES 20mM, Potassium Acetate 150mM, Imidazole 200mM, pH 7). After injection of the column, a wash was done with 92.5% Buffer A and 7.5% Buffer B (15mM imidazole final). Elution was done with 100% Buffer B. Fractions of 5ml were collected. After analysis by SDS-PAGE stained with coomassie, peak fractions 10 to 12 were combined. The samples was injected in a MonoQ column of 5ml. Buffers used where Buffer A (HEPES 20mM, Magnesium Acetate 1mM, pH 7) and Buffer B (HEPES 20mM, Potassium Acetate 1M, Magnesium Acetate 1mM, pH 7). The column was equilibrated with 70% Buffer A and 30% Buffer B. The elution was done with increasing the concentration of Buffer B, 1% per minute during the first 14 minutes and then 5% per minute during the last 5 minutes. Final elution was done with 100% Fractions of 1ml were taken. A coomassie gel was done to find the peak fractions. The preparation turned out to give two different pools, and only the second pool was found to be active for budding assay.

Microsome purification:

Fragments of the ER, known also as microsomes, can be obtained from homogenized cells and are very useful as donor membranes for semi-in vitro reactions or analysis of ER protein and lipid composition (Shimoni and Schekman, 2002). In our studies, wild type yeast strain BY4742 was grown in 1L YPD cultures to densities of 1.5 to 1.8 OD₆₀₀/ml. The cells were collected by centrifugation and treated with lyticase to remove the cell wall. After no more than 30 minutes of treatment, 85% of spheroplasting efficiency was achieved as measured by light absorbance at 600nm. The resulting spheroplasts were collected by centrifugation and frozen at -80°C overnight. Afterwards, the pellet of spheroplast was thawed on ice and resuspend in lysis buffer (HEPES 20mM pH 7.4, EDTA 2mM, sorbitol 0.1M, Potassium Acetate 50mM, DTT 1mM, PMSF 1mM). The spheroplasts were homogenized using a motorized dounce homogenizer (9 strokes), which shears the spheroplasts and release organelles and cytoplasm to the solvent. This homogenate was first subject of a mild centrifugation (5000 xg, 5 min, 4°C) to remove most of the nuclei, plasma membrane and mitochondria, which are discarded as the pellet. The solution is then centrifuged stronger (27,000 xg, 10 min, 4°C) which allows to collect the ER fragments, now microsomes, as a pellet. This pellet is resuspended and microsomes are further purified in a two steps sucrose gradient (bottom layer 1.5M, top layer 1.2M) using ultracentrifugation in swing bucket rotor (100.000 xg, 1 hour, 4°C). Microsomes were collected at the interphase between the two sucrose phases, discarding other membrane aggregates by aspiration. This process usually generated 3.2 mg/ml of proteins as measured by UV light spectrophotometer, which is considered a good working condition for in vitro vesicle formation assay. Microsomes were finally aliquoted and frozen at -80°C.

In vitro vesicle formation assay.

Preparation of microsomes. All steps are done at 4°C except incubation for vesicle generation. Two aliquots of microsomes per budding reaction, including two per negative control, were thawed on ice. Each microsome aliquot was in the range of 3.2 mg/ml of protein. Once the microsomes are thawed, all aliquots are combined in one single siliconized eppendorf. Microsomes were incubated with ATP 1mM at 6°C for 10 minutes and after this placed on ice for 5 minutes. After this, microsomes are carefully washed with 2 volumes of B88 (HEPES 20mM, sorbitol 250mM, Potassium Acetate 150mM, Magnesium Acetate 5mM, pH 6.8) and centrifuged at 19000 xg for 3 minutes. Washes were repeated 3 times. After the

last centrifugation is finished, supernatant was aspirated and resuspended in 200µl per budding reaction. Aliquot 200ul in siliconized tubes, one tube per reaction.

In vitro vesicle formation.

Vesicle formation assay was adapted from (Barlowe et al., 1994; Shimoni and Schekman, 2002). Standard budding reaction was composed of 200µl of microsomes from the same batch (3.2 µg/µl of protein as absorbance by OD₂₈₀), 50µl of B88 buffer without Potassium Acetate, 10µl Sec23/24 (stock at 1.5mg/ml), 15µl of Sec13/31 (stock at 1.5mg/ml), 12µl of Sar1 (stock at 3.3mg/ml) and GTP 1mM (Sigma) previously combined with an ATP regeneration system composed of ATP 1mM (Sigma), GDP-mannose 50µM (Sigma), creatine phosphate 40mM (Sigma), and creatine phosphokinase 2 mg/ml (Sigma C3755-17.5KU). Finally, B88 buffer is added to complete 500µl volume. The mix was softly vortexed and vesicle reaction was started by placing the tubes in a waterbath at 23°C for 25 minutes. To finish the reaction, all tubes were placed in ice for 5 minutes. After this, 5% of each reaction was taken and combined together and labelled as Total fraction. All samples (excluding totals) were centrifuged at 19.000 xg for 3min at 4°C. Afterwards, 450µl of supernatant were taken carefully, avoiding the pellet of microsomes. The pellets were kept at 4°C for the instant or immediately frozen in liquid N₂. The supernatant was divided in two and each half was placed in different ultracentrifuge tubes. All samples were ultracentrifuged at 55.000 rpm for 12 minutes at 4°C in a Beckman TLA 100.3 rotor. Finally, all supernatants were discarded and vesicular fraction was immediately frozen in liquid N2 and stored at -80°C.

Vesicle analysis by western blot.

The vesicular pellet is not visible to the eye and tightly bound to the bottom of the tube after ultracentrifugation, therefore, the pellet of the fraction called "totals" was used as a reference to assess the solubilization of vesicular pellets. Each sample was resuspended in 35µl of 5x Laemmli sample buffer, then boiled for 3 minutes at 95°C and finally vigorously vortexed. The whole process was repeated 3 times or until "totals" sample was fully dissolved. Then, 5µl of each sample were used to analyze the vesicular markers by SDS-PAGE at 12.5% acrylamide concentration (eventually 10%) (Laemmli, 1970). We used rabbit antibodies against COPII markers and ER resident proteins. The analysis of several of these proteins in the same western blot allowed us to judge the efficiency of the vesicle formation assay by comparison between negative and positive control reactions and in comparison with the fraction called "totals", equivalent to 5% of the original protein content in the microsomal batch.

Lipid extraction and analysis.

Yeast sample collection and extraction from yeast cultures incubated at 24°C and 33°C.

Strains YPH499, SMY80 and SMY80 transformed with PLB3 plasmid were grown on selective media overnight at 24°C. At 0.5 OD $_{600}$ /ml cells were collected and resuspended in YPD (For 1L: glucose 20g, Bacto peptone 10g, Bacto yeast extract 20g, MES hydrate 1.95g and 40mg each of Tryptophan, Uracil and Adenine) and each culture was split in two. One half was left growing at 24°C while the other half was placed at 33°C. Cells were collected when cultures reached 1 OD $_{600}$ /ml and processed for lipid extraction. The cultures were transferred to 50 ml FALCON tubes and cellular metabolism was stopped with trichloroacetic acid (5% final). Tubes were incubated for at least 10 minutes on ice and after centrifuged for 5 minutes at 800g. Cells were washed with 10ml 5% TCA and centrifuged for 5 minutes at 800g. The pellet was resuspended in 5 ml water and the appropriate amount to have 25 OD (1 OD = 10 8 cells) was transferred into a 10 ml glass tubes. Then centrifuged for 5 minutes at 800g. The supernatant was removed and frozen in the tubes at -80°C.

The lipids were extracted as previously described (Guan et al., 2010) the pellets were thawed and 500µl glass beads were added together with 25 ml of internal standard mix (7.5 nmol of 17:0/14:1 PC, 7.5 nmol of 17:0/14:1 PE, 6.0 nmol of 17:0/14:1 PI, 4.0 nmol of 17:0/14:1 PS purchased from Avanti Polar Lipids [Alabaster, AL]). Then, 1.5 ml extraction solvent (ethanol, water, diethyl ether, pyridine, and 4.2 N ammonium hydroxide [15:15:5:1:0.018, vol/vol]) was added. The sample was vortexed for 6 minutes on a multi vortexer (Labtek International, Christchurch, New Zealand). Samples were incubated for 20 minutes at 60° C and after were centrifuged for 5 minutes at 800g. The supernatant was transferred to a clean 13 mm glass tube (Corning) with a Teflon-lined cap. The extraction was repeated once by adding extraction solvent to the beads. The samples were dried under a flow of N_2 and store at -80° C.

The analysis was done as described (da Silveira Dos Santos et al., 2014) with minor modifications. Glycerophospholipids were analyzed by high resolution mass spectrometry, a Q Exactive Hybrid Quadrupole-Orbitrap Mass Spectrometer (Thermo Scientific) was used. Lipid extracts were dissolved in 500 µl of chloroform:methanol (1:1, vol/ vol) and diluted two times in 5 mM ammonium acetate in chloroform:methanol:water (2:7:1, vol/vol/vol) for both positive- and negative-ion-mode mass analysis. Samples were analyzed by direct infusion. Positive-ion-mode analysis was performed using scan range m/z = 650–800 (for monitoring PC and PE). Negative-ion-mode analysis was performed using scan range m/z = 700–850 (for monitoring PI and PS). Lipid species were identified according to their m/z, and their abundance was calculated by their signal intensities relative to internal standards.

Lipid extraction and analysis of cells, microsomes and COPII vesicles.

Strain BY4742 was used for all experiments related to *in vitro* vesicle formation assay. Yeast were grown in YPD (For 1L: glucose 20g, Bacto peptone 10g, Bacto yeast extract 20g, MES hydrate 1.95g) to \sim 1.5 OD₆₀₀/ml and were processed to spheroplasts. Before adding lyticase to the sample, an aliquot of 25 OD (1 OD = 10^8 cells) was taken and frozen with liquid N₂ when lyticase reaction was finished. Microsome pellets (\sim 350µg in proteins mass) were used for glycerophospholipid analysis. As for vesicles and budding reaction backgrounds, at the end of budding assay the sample was divided in two and one aliquot was used for glycerophospholipid analysis.

MTBE lipid extraction (Loizides-Mangold et al., 2012; Matyash et al., 2008) with some modifications was done for all samples. Samples were thawed on ice and resuspended in 100µl of water. 360 µl of methanol and a mix of internal standards was added (7.5 nmol of 17:0/14:1 PC, 7.5 nmol of 17:0/14:1 PE, 6.0 nmol of 17:0/14:1 PI, 4.0 nmol of 17:0/14:1 PS purchased from Avanti Polar Lipids [Alabaster, AL]). 200µl of glass beads were added to cell samples. Samples were vortexed and 1 ml of MTBE was added. Samples were placed for 10 min on a disruptor genie at 4°C (Scientific industries, Bohemia, NY). After vortexing, samples were transferred to 2ml Eppendorf tubes and completed volumes were completed with 200µl of MTBE. This was followed by an incubation for 1 h at room temperature (RT) on a shaker. Phase separation was induced by addition of 200 µl MS-grade water. After 10 min of incubation at RT samples were centrifuged at 1,000 g for 10 min. The upper (organic) phase was transferred into a 13 mm glass tube (Corning) with a Teflon-lined cap and the lower phase was re-extracted with 400 I of a MTBE/MeOH/H₂O mixture (10:3:1.5). Samples were vortexed, incubated for 10 min at RT, and centrifuged for 10 min at 1000 g. The upper phase was collected and the combined organic phases were dried in a CentriVap Vacuum Concentrator (Labconco, MO).

The analysis of glycerophospholipids was done as described for the previous extraction (see Yeast sample collection and extraction from yeast cultures incubated at 24°C and 33°C).

COPII reconstitution assays.

GUV electroformation.

Major-minor mix was done as described in (Daum et al., 2014; Matsuoka et al., 1998) with few modifications. Mixes of 2mg/ml of lipids were combined by mol percent: 34.4% Glycerophospholipids 1,2-dioleoyl-sn-glycero-3-phosphocholine (DOPC), 14.8 % 1,2-dioleoyl-sn-glycero-3-phosphoethanolamine (DOPE), 5.4% soy L- α -phosphatidylinositol (PI), 5.4% 1,2-dioleoyl-sn-glycero-3-phospho-L-serine (DOPS), 3.4% 1,2-dioleoyl-sn-glycero-3-phosphate (DOPA), 1.5% porcine brain L- α -phosphatidylinositol-4-phosphate from

porcine brain [PI(4)P], 0.5% porcine brain L- α -phosphatidylinositol-4,5-bisphosphate [PI(4,5)P2], 1.3% 1,2-dioleoyl-sn-glycero-3-(cytidine diphosphate) (CDP-DAG), 33% ovine wool cholesterol and 0.05% 1,2-dioleoyl-sn-glycero-3-phosphoethanolamine-N-(lissamine rhodamine B sulfonyl) were purchased from Avanti Polar Lipids (Alabaster, AL). When GUVs were prepared with lysophospholipids, 10% of DOPC was substituted with soy L- α -lysophosphatidylinositol (LysoPI).

Lipid mixes were deposited (40µg) on two indium-tin oxide coated (ITO) slides and dried for 30min at 30°C in a vacuum chamber. The ITO slides were sealed one to each other using a silicone O-ring as spacer, opened to introduce 200µl sucrose buffer (500mM adjusted to 592 mOsm) and later sealed with kwik-cast silicone sealant (Sarasota, FL). GUVs were electroformed (1V, 10Hz) for 2 hours at room temperature (~23°C). After the electroformation, the chamber was directly placed at 4°C. Eventually, GUVs were pipetted into a siliconized eppendorf tube and stored at 4°C.

COPII reconstitution:

COPII proteins were purified from yeast strains as described before. Sar1 was chemically labelled at primary amines with Atto 647 (Atto-tec product no. AD 647N-3) and Sec13/31 was labelled similarly with TFP-Alexa-488 (Life technologie product no. A37563). The purified proteins were mixed in B88 buffer (HEPES 20mM, sorbitol 250mM, Potassium Acetate 150mM, Magnesium Acetate 5mM, pH 6.8). Final concentrations were Sar1-Atto647 (0.75 μ g/ μ l), Sec23/24 (0.25 μ g/ μ l), Sec13/31 (0.18 μ g/ μ l) and Sec13/31-Alexa488 (0.18 μ g/ μ l). Sar1 was activated with 2.5mM EDTA in low Mg²⁺ B88 and GTP γ S 1mM. Approximately 5 μ l-10 μ l of crude GUVs preparation were added to the osmolarity-adjusted protein solutions. Reconstitution of COPII with GUVs proteins were incubated at room temperature (<23°C) in a microfluidic chamber (ibidi μ -Slide) precoated with BSA prior to the experiment.

Microscopy was performed using a Nikon Eclipse Ti confocal spinning disc microscope with 100x magnification. Images were analyzed with Fiji.

Barlowe, C., Orci, L., Yeung, T., Hosobuchi, M., Hamamoto, S., Salama, N., Rexach, M.F., Ravazzola, M., Amherdt, M., and Schekman, R. (1994). COPII: a membrane coat formed by Sec proteins that drive vesicle budding from the endoplasmic reticulum. Cell 77, 895–907.

Daum, S., Krüger, D., Meister, A., Auerswald, J., Prinz, S., Briggs, J.A.G., and Bacia, K. (2014). Insights from reconstitution reactions of COPII vesicle formation using pure components and low mechanical perturbation. Biol. Chem. 395, 801–812.

Guan, X.L., Riezman, I., Wenk, M.R., and Riezman, H. (2010). Yeast lipid analysis and quantification by mass spectrometry. Methods Enzymol. *470*, 369–391.

Laemmli, U.K. (1970). Cleavage of Structural Proteins during the Assembly of the Head of Bacteriophage T4. Nature 227, 680–685.

Loizides-Mangold, U., David, F.P.A., Nesatyy, V.J., Kinoshita, T., and Riezman, H. (2012). Glycosylphosphatidylinositol anchors regulate glycosphingolipid levels. J. Lipid Res. *53*.

1522-1534.

Matsuoka, K., Orci, L., Amherdt, M., Bednarek, S.Y., Hamamoto, S., Schekman, R., and Yeung, T. (1998). COPII-coated vesicle formation reconstituted with purified coat proteins and chemically defined liposomes. Cell *93*, 263–275.

Matyash, V., Liebisch, G., Kurzchalia, T.V., Shevchenko, A., and Schwudke, D. (2008). Lipid extraction by methyl-tert-butyl ether for high-throughput lipidomics. J. Lipid Res. 49, 1137–1146.

Okamoto, M., Kurokawa, K., Matsuura-Tokita, K., Saito, C., Hirata, R., and Nakano, A. (2012). High-curvature domains of the ER are important for the organization of ER exit sites in Saccharomyces cerevisiae. J. Cell Sci. *125*, 3412–3420.

Shimoni, Y., and Schekman, R. (2002). Vesicle budding from endoplasmic reticulum. Methods Enzymol. *351*, 258–278.

da Silveira Dos Santos, A.X., Riezman, I., Aguilera-Romero, M.-A., David, F., Piccolis, M., Loewith, R., Schaad, O., and Riezman, H. (2014). Systematic lipidomic analysis of yeast protein kinase and phosphatase mutants reveals novel insights into regulation of lipid homeostasis. Mol. Biol. Cell *25*, 3234–3246.